



SCHOOL of  
GRADUATE STUDIES  
EAST TENNESSEE STATE UNIVERSITY

East Tennessee State University  
Digital Commons @ East  
Tennessee State University

Electronic Theses and Dissertations

Student Works

12-2010

# Studies on the Preparation and Luminescence Properties of Cadmium Selenide Quantum Dots, Their Immobilization, and Applications.

Travis Justin Heath

*East Tennessee State University*

Follow this and additional works at: <https://dc.etsu.edu/etd>

 Part of the [Nanoscience and Nanotechnology Commons](#)

## Recommended Citation

Heath, Travis Justin, "Studies on the Preparation and Luminescence Properties of Cadmium Selenide Quantum Dots, Their Immobilization, and Applications." (2010). *Electronic Theses and Dissertations*. Paper 1750. <https://dc.etsu.edu/etd/1750>

This Thesis - Open Access is brought to you for free and open access by the Student Works at Digital Commons @ East Tennessee State University. It has been accepted for inclusion in Electronic Theses and Dissertations by an authorized administrator of Digital Commons @ East Tennessee State University. For more information, please contact [digilib@etsu.edu](mailto:digilib@etsu.edu).

Studies on the Preparation and Luminescence Properties of Cadmium Selenide Quantum Dots,  
Their Immobilization, and Applications

---

A thesis  
presented to  
the faculty of the Department of Chemistry  
East Tennessee State University

---

In partial fulfillment  
of the requirements for the degree  
Master of Science in Chemistry

---

by  
Travis Justin Heath  
December 2010

---

Dr. Chu-Ngi Ho, Chair  
Dr. Jeffrey Wardeska  
Dr. Peng Sun

Keywords: Cadmium Selenide, Nanoparticles, Quantum Dots, Sol-Gel, Fluorescence,  
Chemiluminescence

## ABSTRACT

Studies on the Preparation and Luminescence Properties of Cadmium Selenide Quantum Dots,  
Their Immobilization, and Applications

by

Travis Justin Heath

Quantum dots are semiconductive particles whose properties are highly influenced by the presence of at least one electron. Cadmium selenide quantum dots were synthesized via colloidal synthesis. Contrary to previous preparations, more focus was placed on the temperature rather than the duration of time at which they form. A series of colored solutions were obtained because the excited quantum dots of various sizes emitted specific wavelengths of light. The emission spectra showed that the temperature-dependent quantum dots were successfully synthesized. The quantum dots were also immobilized on various surfaces, and the luminescence properties were examined. The quantum dots that were immobilized in sol-gels through chemiluminescence (CL) analyses were found to be stable and were able to maintain their luminescence properties with extensive uses and long-term storage. Linear calibration curves were obtained for concentrations of hydrogen peroxide from  $1.75 \times 10^{-4}$  M to  $1.75 \times 10^{-2}$  M in TCPO-CL.

## DEDICATION

To my loving parents, Ronald and Syrilda Heath

## ACKNOWLEDGEMENTS

First acknowledgements go to my Lord and Savior Jesus Christ. Without Him, none of this would even be possible. Through my faith in Him, I was able to complete this portion of my higher education with no stress or anxiety. Therefore, all glory, honor, and praise belong to Him.

I would like to thank Dr. Chu-Ngi Ho for his professional guidance and encouragement throughout this entire experience. He challenged me, was always available to answer any questions that I had, and always had an encouraging word to say to keep me motivated.

I would also like to thank Dr. Jeffery Wardeska and Dr. Peng Sun for serving on my thesis committee. They provided me with constructive feedback in critiquing my thesis. The entire faculty and staff of the chemistry department have truly helped me as well. They graciously paid for my higher education and prepared me future challenges.

I am extremely grateful for my parents, Ronald and Syrilda Heath; my brother, Christopher Heath; and my entire family. Words cannot express how much I love and appreciate my family. They encouraged me by letting me know that I will do well and can be successful in anything in life. Through every action that they did, they let me know what love truly is.

Last but certainly not least, I would like to thank my friends and classmates for all that they did to help me get to where I am today. A special recognition goes to Mrs. Barbara Rasnick and Shelley Van Cleve. The two of them helped me remain stress-free by taking time to listen to my concerns and offering advice. The both of them truly have a special place in my heart.

May God bless all of you both now and always.

## TABLE OF CONTENTS

	Page
ABSTRACT.....	2
DEDICATION.....	3
ACKNOWLEDGEMENTS.....	4
LIST OF TABLES.....	10
LIST OF FIGURES.....	11
Chapter	
1. INTRODUCTION.....	13
Nanoparticles.....	13
History of Nanoparticles.....	14
Fullerenes.....	15
Semiconductor Nanocrystals.....	15
Other Nanoparticles.....	16
Quantum Dots.....	17
Quantum Dot Properties.....	18
Size Properties.....	18

Surface Properties.....	18
Quantum Dot Applications.....	19
Industrial Field.....	19
Medical Field.....	19
Technological Field.....	20
<b>2. PROPERTIES OF CdSe QUANTUM DOTS AND LUMINESCENCE</b>	
<b>TECHNIQUES.....</b>	<b>21</b>
CdSe Quantum Dots.....	21
Synthetic Procedures of Quantum Dots.....	21
Vapor Deposition.....	22
Molecular Self-Assembly.....	22
Colloidal Synthesis.....	23
Luminescence Techniques.....	23
Principle of Fluorescence.....	24
Principle of Chemiluminescence.....	27
Peroxyoxalate Chemiluminescence.....	28
Applications of Peroxyoxalate Chemiluminescence.....	30
Research Proposal.....	30

3. EXPERIMENTAL PROCEDURE.....	32
Reagents Used.....	32
Preparation of Stock Solutions.....	33
Selenium Precursor Solution.....	33
Imidazole Solution.....	33
Hydrogen Peroxide Solution.....	33
Synthesis of CdSe Quantum Dots.....	33
Preparation of Working Solutions.....	34
Preparation of Quantum Dot Solutions for Linearity Studies.....	34
Preparation of Quantum Dot Solutions for Obtaining an Emission Spectrum.....	34
Preparation of Quantum Dot Solutions for Immobilization Studies...	34
TCPO Solution.....	35
Preparation of Hydrogen Peroxide Solutions for Linearity Test.....	35
Preparation of the Immobilized Quantum Dots.....	35
Preparation of the Sol-Gels and Immobilization of Quantum Dots.....	35
Preparation of TCPO.....	36



Procedure of Measurement.....	36
Optimization of Imidazole Study.....	36
Reproducibility Studies.....	37
Linearity Study Using One Sol-Gel.....	37
Linearity Study Using Multiple Sol-Gels.....	37
Linearity Study Using Crushed Sol-Gels.....	38
Instrumentation.....	38
Instrumentation for Fluorescence.....	38
Instrumentation for Chemiluminescence.....	38
4. RESULTS AND DISCUSSION.....	40
Fluorescence Studies of the Quantum Dot (QD) Solutions.....	40
Time-Based QD Synthesis.....	40
Temperature-Based QD Synthesis.....	40
Effect of QD Size on the Emission of Light.....	41
Emission Spectra of QD.....	42
Linearity Studies of Fluorescence Signal with Concentration of QD.....	44
QD Immobilization by Adsorption Studies.....	45

Feasibility Studies of Sol-Gel Immobilized QD in TCPO-CL.....	51
Optimization of Amount of Imidazole Catalyst.....	52
Reproducibility Studies.....	53
Linearity Studies of CL Intensity with H <sub>2</sub> O <sub>2</sub> Concentration Using Sol-Gel Immobilized QD.....	55
One Sol-Gel.....	55
Multiple Sol-Gels.....	57
Crushed Sol-Gels.....	59
5. CONCLUSION.....	63
REFERENCES.....	66
VITA.....	73

## LIST OF TABLES

Table	Page
1. Color of CdSe QD Solutions Synthesized by Heating Cd and Se Precursors to Different Temperatures and When Exposed to Ultraviolet Light.....	42
2. Result of Maximum Emission Wavelength Peak with Varying Temperatures.....	44
3. Measurement of CdSe Quantum Dot Solution Fluorescence Prepared at 195 °C for Linearity Study with an Excitation and Emission Wavelengths of 400 nm and 535 nm, Respectively.....	45
4. Results of the Optimization of Imidazole for TCPO-Hydrogen Peroxide CL Reaction.....	52
5. Results of Reproducibility Study of Proposed CL Method Using Five Different $8.75 \times 10^{-4}$ M Hydrogen Peroxide Solutions.....	54
6. Results of Reproducibility Study of Proposed CL Method Using a Single Sol-Gel with Immobilized QD.....	55
7. Results of Linearity Studies of CL Intensity with Hydrogen Peroxide Using a Single Sol-Gel with Immobilized QD.....	56
8. Results of Linearity Studies of CL Intensity with Various Concentrations of Hydrogen Peroxide Using Multiple Sol-Gels with Immobilized QD.....	58
9. Results of Linearity Studies of CL Intensity with Various Concentrations of Hydrogen Peroxide Using Crushed Sol-Gels with Immobilized QD.....	60

## LIST OF FIGURES

Figure	Page
1. A simplified Jablonski diagram showing the various electronic and vibronic levels and the processes possible.....	25
2. The chemical structure of bis(2,4,6-trichlorophenyl) oxalate, TCPO.....	29
3. Schematic diagram of the fluorescence spectrophotometer.....	39
4. Schematic diagram of the chemiluminescent instrumentation.....	39
5. Plot of the fluorescence spectrum of QD synthesized at 210 °C ranging from 480 nm to 590 nm at 5 nm intervals.....	43
6. Plot of the fluorescence intensity of 195 °C QD solution dissolved in cyclohexane in 5-mL volumetric flasks.....	45
7. Plot of the fluorescence spectrum of QD synthesized at 160 °C ranging from 480 nm to 550 nm at 5 nm intervals.....	46
8. Plot of the fluorescence spectrum of immobilized 195 °C QD chromosorb and glass bead solids.....	47
9. Plot of the fluorescence spectrum of 195 °C decanted QD solution from immobilized chromosorb and glass bead solids.....	47
10. Plot of the fluorescence spectrum of immobilized 160 °C QD silica gel and alumina solids.....	48
11. Plot of the fluorescence spectrum of 160 °C decanted QD solution from immobilized silica gel and alumina solids.....	49
12. Plot of the fluorescence spectrum of 160 °C decanted QD solution from immobilized alumina with mesh sizes of 100-150 mesh and 150-200 mesh.....	51

Figure	Page
13. Plot of the results of the optimization of imidazole experiment for the TCPO (7.5 mg/mL) - hydrogen peroxide ( $8.75 \times 10^{-3}$ M) reaction.....	53
14. Plot of the average duplicate CL measurements on each separately prepared triplicate hydrogen peroxide solution using 3.0 mL of TCPO, 50 $\mu$ L of imidazole, and a single sol-gel with immobilized QD.....	57
15. Plot of the linearity curve of the average duplicate CL measurements on each separately prepared triplicate hydrogen peroxide solution using 3.0 mL of TCPO, 50 $\mu$ L of imidazole, and a single sol-gel with immobilized QD.....	57
16. Plot of the average triplicate CL measurements on each hydrogen peroxide solution using 3.0 mL of TCPO, 50 $\mu$ L of imidazole, and multiple sol-gels with immobilized QD.....	58
17. Plot of the linearity curve of the average triplicate CL measurements on each hydrogen peroxide solution using 3.0 mL of TCPO, 50 $\mu$ L of imidazole, and multiple sol-gels with immobilized QD.....	59
18. Plot of the average duplicate CL measurements on each hydrogen peroxide solution using 3.0 mL of TCPO, 50 $\mu$ L of imidazole, and crushed sol-gels with immobilized QD.....	60
19. Plot of the linearity curve of the average duplicate CL measurements on each hydrogen peroxide solution using 3.0 mL of TCPO, 50 $\mu$ L of imidazole, and crushed sol-gels with immobilized QD.....	61
20. Plot of the linearity curve of the average duplicate CL measurements on each hydrogen peroxide solution using 3.0 mL of TCPO, 50 $\mu$ L of imidazole, and crushed sol-gels with immobilized QD.....	62

## CHAPTER 1

### INTRODUCTION

Nanotechnology is the study of material of atomic or molecular scale, more specifically, of nano scale. In nanotechnology one studies the synthesis and properties of particles with a diameter of 100 nm or smaller. This particular field of science has been a topic of interest in recent decades. Much research has gone into synthesizing materials and developing devices to analyze these materials because the main idea behind nanotechnology is to synthesize matter reproducibly and with control on the nano scale. Working with bulk material is becoming more economically challenging. The various types of analysis performed on the bulk material are very time consuming and require more financial support. However, nanotechnology allows one to manipulate the properties of the material. As a result, chemists can overcome the challenges by addressing the issues associated with the bulk material on a very small scale.

#### Nanoparticles

When studying nanotechnology, chemists focus much of their attention on analyzing materials on the nano scale, also known as nanoparticles. Nanoparticles are particles with diameters of 100 nm or smaller (1). Nanoparticles are aggregates of multiple atoms or molecules. Therefore, they are larger than an individual atom or molecule but are much smaller than the corresponding bulk material. Their sizes affect the material's chemical and physical properties. In addition, nanoparticles exist in diverse morphologies, including tubes, cylinders, spheres, and core/shell structures (1, 2). The shape of the nanoparticles is based upon how it is synthesized for specific applications. Moreover, nanoparticles have various chemical

compositions. The most common include organics, polymers, silicates, metals, metal oxides, and nonoxide ceramics (1).

Nanoparticles are designed and synthesized for specific applications. These applications are based upon the dispersion medium that contains the nanoparticles, the dispersion state, and the miscellaneous surface modifications involved (1). Some nanoparticles are immobilized into sol-gels and other solid matrices. Other nanoparticles remain dispersed in liquid solutions and can be conformed into gaseous media. The particles can be dispersed individually, or they can be dispersed as ordered structures. Also, the individual particles can form aggregated or agglomerated states. Nanoparticles can also undergo surface modifications and are used in numerous areas of human life. For instance, they have been grafted and adsorbed to surfactants (1) and polymers (3). Thus, nanoparticles have been used in the cosmetic, environmental, medical, and technological fields (1, 4).

### History of Nanoparticles

The first concepts of nanotechnology were introduced in the late 1950s by Richard Feynman, a former physicist and Nobel Laureate at California Institute of Technology (5). Feynman noted that working with bulk material was becoming more challenging. Therefore, he looked into working with materials on a nano scale in order to manipulate their properties for the desired applications. He also researched the development of devices that would function on such a small scale. Then, an engineer named Eric Drexler studied these concepts of nanotechnology in greater depth (6). Much research has since gone into improving the properties of nano-scaled devices. All of this research led to the discovery of fullerenes (7), semiconductor nanocrystals (8), and other nanoparticles (9-14).

## Fullerenes

The study of nanoparticles began with the discovery of fullerenes, a class of compounds of hollow-caged carbon clusters. Fullerenes are molecules that are composed completely of carbon atoms. They were discovered in the 1980s by Robert Curl, Jr. and Richard Smalley (7) of Rice University in Houston, Texas and Harold Kroto (15) of Sussex University in the United Kingdom. The most abundant fullerene is  $C_{60}$ . The spherical structure that is identical to that of a soccer ball was designed by an architect named Buckminster Fuller (7). Therefore,  $C_{60}$  was named Buckminsterfullerene. Curl, Kroto, and Smalley were awarded the Nobel Prize in 1996 for their achievements. After this discovery, carbon nanotubes and onion-shaped structures were synthesized. These structures established a connection between fullerenes and graphite. Alkali metal salts can be synthesized from fullerenes and are used in the study of superconductive materials. In addition, fullerenes are also used in biological and medical applications (7).

## Semiconductor Nanocrystals

In the mid-1980s, Louis Brus, a physical chemist at Columbia University, began studying semiconductor particles (8). He began his research by studying how energy flows in molecules in solid material. Laser beams were radiated through the solid material and excited the embedded impurity molecules. As various color changes were observed from the emitted light, property differences between the excited and relaxed states were noted (16). After studying solid materials, Brus focused his research on room temperature solutions. Using semiconductive materials, he excited electrons from the valence band to the conduction band and observed the changes in the band gap energy (17). As Brus collaborated with other researchers, it was discovered that there was a relationship between the band gap and the size of the particles (18).



These particles, also called nanocrystals, were used in further research of smaller semiconductors (19, 20).

In the late 1980s, Mark Reed, a physical chemist at Yale University, also researched semiconductor nanocrystals. He referred to these nanocrystals as quantum dots because they contain some quantum mechanical components (21). Reed wanted to link quantum dots in circuits so that they could be used in computers and other electrical devices. The goal was to produce faster and smaller computer chips and more useful quantum devices.

### Other Nanoparticles

Zinc oxide and titanium dioxide nanoparticles have been synthesized and used in sunscreen lotion to protect the skin from ultraviolet radiation (9). In the past, the sunscreen lotion would appear white on the skin. However, with recent developments, the lotion remains colorless on the skin while the nanoparticles retain their sunscreen properties. Both the zinc oxide and titanium dioxide nanoparticles remain on the surface of the skin, where the nonviable skin cells are located, and absorb the ultraviolet radiation. There have been concerns that the nanoparticles adsorb to viable skin cells under the surface of the skin, which could lead to skin cancer when exposed to the ultraviolet light. However, current research suggests that the nanoparticles remain on the outside surface of the skin (9).

Silver nanoparticles have been synthesized and used in fighting bacteria, viruses, and fungi (10). In many cases, bacteria, viruses, and fungi behave similarly. They use enzymes to carry out chemical reactions necessary to produce oxygen gas, which is essential for their survival. Antibiotic drugs have been used to fight against them, but they are becoming increasingly resistant. However, the silver nanoparticles interact with living cells and increase

their antibacterial efficiency. In addition, they destroy the enzymes and suffocate the bacteria, virus, and fungi so that they do not infect the surrounding tissue (10).

Gold nanoparticles have been synthesized and used in the diagnosis of genetic diseases and mutations (11). The gold nanoparticles are attached to the oligonucleotides. The nanoparticles emit light after being exposed to radiation. Through fluorescence analyses, the genetic disease or mutation can be detected and treated immediately. By using gold nanoparticles, simpler instrumentation is involved, and reliable results are obtained (11).

As more research was conducted, other types of nanoparticles were discovered. For instance, liposomes were synthesized and used in both the cosmetic and pharmaceutical industries (12, 13). Also, nanoshells were developed, which are spherical particles surrounded by a protective coating. These nanoparticles are used in medicine, particularly in treating cancer (14).

### Quantum Dots

One form of nanoparticles studied is quantum dots. Quantum dots are inorganic semiconductor nanocrystals whose electrons highly influence their physical and chemical properties (22). They are synthesized from II/VI semiconductors (23-25). Although they are composed of hundreds and even thousands of atoms, they behave like a single atom (26, 27). Quantum dots are considered to be hydrophobic particles because their surfaces are composed of nonpolar coordinating ligands. However, when coated with a more polar shell, they can dissolve in water (27).

The presence of electrons in both the relaxed and excited states influences the conductivity of the quantum dots. Electrons exist in their ground states in the valence band (8).

When an electron absorbs radiation from an energy source, it jumps to an excited state in the conduction band, leaving a hole in the ground state orbital. As the electron returns to its ground state, it emits energy at a specific wavelength of light (22). Also, the size and surface properties of the quantum dots affect the emission wavelength (8).

### Quantum Dot Properties

Size Properties. Small quantum dots are not very stable because they have high surface areas per unit volume. Therefore, they have a tendency to grow (8). The size of the quantum dots affects the band gap energy. With larger quantum dots, the energy levels are closer together and require less energy to excite an electron to an excited state. As a result, when the electron returns to its ground state, light of a specific wavelength is emitted (26). Larger quantum dots emit longer wavelengths of light, toward the red end of the visible spectrum, while smaller quantum dots emit shorter wavelengths of light, toward the blue end of the visible spectrum (28, 29). In addition, when they are bound to metals, the quantum dot size influences magnetic behavior and sintering and melting temperatures of the metals. The thermal conduction properties of quantum dots are also influenced. Thermal conductivity is enhanced as the size of the quantum dots increase (1).

Surface Properties. The surface chemistry of quantum dots is important as well. Quantum dots enhance catalytic activity because they have a high surface area per unit volume. When immobilized in solid material, the surface areas produce strong interactions between the solid matrix and the quantum dots. For example, when they are immobilized in a polymer, the heat deflection and glass transition temperatures of the polymer are increased, and as a result, the

flammability of the polymer increases. Also, the elasticity of the polymer increases without a significant loss in strength (1).

### Quantum Dot Applications

Quantum dots are used in several areas of human activity, such as in the industrial, medical, and technological fields.

Industrial Field. Quantum dots are slowly replacing organic dyes used in tissue staining. When comparing quantum dots and organic dyes, researchers examine their optical properties (23, 30, 31). Similar to quantum dots, organic dyes absorb radiation to excite an electron and emit energy as the electron returns to its ground state. However, the use of organic dyes is becoming more challenging for several reasons. For instance, photobleaching can occur with most organic dyes after they have been exposed to light for an extended period of time. As a result, it becomes more difficult to observe cellular processes and analyze fluorescent characterization (23, 26, 32). The colors produced by the quantum dots last for weeks or longer, which provide more time for observation and characterization (23, 33, 34). In addition, quantum dots are replacing organic dyes because they are 10-times larger than organic dyes; this permits them to shine brighter (35). Finally, organic dyes fluoresce at distinct laser wavelengths, and one color is observed at a time. On the other hand, quantum dots emit light of different wavelengths when excited by one wavelength of light (26). Quantum dots will not completely replace organic dyes because fluorescence measurements become difficult when the size- and surface-dependent variables and the decaying behavior of the quantum dots are introduced (27, 36, 37).

Medical Field. Quantum dots are used in cancer research (26). One particular area of research is *in vivo* imaging. When cancer cells move in the body, they consume the normal cells

and leave a dark path behind them. Consequently, it becomes difficult to detect where the cancer cells have spread. However, these cells can devour quantum dots as well. As the cells travel throughout the body, they can be seen when exposed to a specific wavelength of light. Also, quantum dots are used in drug-carrier research (35, 38, 39). Researchers have conjugated quantum dots to antibodies to recognize cancer cells (26). Now, they want to develop a successful method to kill the cancer cells. Researchers want to inject quantum dots with specific toxins and protect them with different coatings. They would release the toxin when exposed to a laser light and exterminate the cancer cells upon interaction. The size of the quantum dots could prevent them getting beyond the surface of tissue. Also, the energy of emissions could cause tissue damage (26). Further research is currently underway to understand all this.

Technological Field. Quantum dots are used in the advancement of technology. They are incorporated in more efficient circuit chips and smaller, more powerful transistors for computers (40, 41). As a result, the speed at which computers function would increase, and overheating problems would be minimized. Quantum dots are also found in lasers and sensors. They are highly sensitive and provide high power and great stability with minimal electrical current required. These applications are currently under review in order to improve the functionality of the quantum dots (40).

## CHAPTER 2

### PROPERTIES OF CdSe QUANTUM DOTS AND LUMINESCENCE TECHNIQUES

#### CdSe Quantum Dots

Cadmium is a transition metal with an atomic number of 48 and a relative atomic mass of 112.4 g/mol. It forms stable bonds with selenium to produce cadmium selenide, CdSe. CdSe quantum dots, also known as II/VI semiconductors, have been produced via multiple synthetic procedures (42).

CdSe quantum dots have been well-studied due to their numerous attractive properties. For example, they are stable in both liquid and solid states, particularly in sol-gels (1). The sizes of the quantum dots approximately range from 1 nm to 10 nm (43, 44). They emit various wavelengths of light ranging from yellow to red. When exposed to ultraviolet light, they luminesce from blue to yellow (29). When kept in the dark, the quantum dots remain stable for days and even months (43). During this time period, they retain the ability to emit light. Although these properties are the primary focus, CdSe quantum dots are toxic. Cadmium is a carcinogen, and both cadmium and selenium are toxic by contact and inhalation. Therefore, appropriate protective equipment and proper disposal should always be considered (27, 45).

#### Synthetic Procedures of Quantum Dots

There are many methods for synthesizing quantum dots. They are categorized as solid, liquid, or gas phase processes. The most popular procedures include vapor deposition, molecular self-assembly, and colloidal synthesis (1).

## Vapor Deposition

Vapor deposition involves a supersaturated vapor being deposited on a solid surface. A supersaturated vapor is achieved by heating a metal and releasing the vapors into a carrier gas phase that usually consists of oxygen gas. While in the gas phase, nucleation takes place either homogeneously or heterogeneously. Homogeneously, the nuclei grow by collision and condensation to produce the quantum dots (1). Heterogeneously, the vapor is condensed into liquid molecular clusters using additional amounts of the cooled carrier gas and exposed to a solid surface (46). As time elapses, the nuclei grow on the surface and give rise to quantum dots. The vapor deposition method has been used to synthesize a variety of metal oxide nanoparticles, such as titanium (II) oxide and zinc oxide (1, 47). In addition, it has been an inexpensive process used in window glass coating and micro-electronics industries. Researchers have gathered information about the environments in which quantum dots grow and the crucial factors that enhance or limit their growth (40, 48, 49). However, the vapor deposition method is mainly used for coating and immobilizing quantum dots (47).

## Molecular Self-Assembly

The molecular self-assembly method is a spontaneous process in which the quantum dots are synthesized from molecules. This method is mainly used for creating polymeric nanoparticles from amphiphilic block copolymers. It is dependent upon the block copolymer, the solvent, and the self-assembly conditions (1, 3). Thermodynamically stable nanoparticles, such as metal sulfides and metal selenides, have been synthesized as well. They have been precipitated by reacting surfactants, such as dihexadecyl phosphate and dipalmitoyl phosphatidyl ethanolamine, with an aqueous solution of a metal salt, and a reactant gas (46). With the

molecular self-assembly method, both the size and the shape of the nanocrystals can be controlled. However, the highly toxic surfactants used in this process give rise to environmental concerns (46).

### Colloidal Synthesis

Colloidal synthesis is the most popular and most efficient method to produce quantum dots (43). It is simple and can be used to synthesize large quantities of high-quality nanoparticles at minimal costs (50-52). In addition, the shape and size (46, 53) and the rate at which they grow (54) can be controlled quite easily. In a colloidal synthesis, an inorganic compound reacts with organic solvents, such as trioctylphosphine (TOP) and oleic acid (48, 55). The quantum dots are precipitated when a precursor solution is added to the mixture at temperatures ranging from 100 °C to 350 °C (46, 54). To synthesize particles of various sizes, aliquots of the solution can be removed from the reacting mixture solution at different times while being heated. The colloidal quantum dots do not settle out of the solution. Therefore, they cannot be easily filtered (29).

### Luminescence Techniques

Numerous analytical techniques have been applied to nanotechnology. Fluorescence and chemiluminescence are the most powerful and widely-used luminescent techniques. With fluorescence, molecules absorb light and become excited. They emit photons of light as the de-excitation process takes place. Fluorescence has a wide linear dynamic range and is highly sensitive and selective. In addition, it is used to for both qualitative and quantitative analyses. Chemists find fluorescence to be an informative yet simple technique.



Chemiluminescence is a luminescent technique in which a species is produced and simultaneously excited by a chemical reaction and emits light as it returns to its ground state. Chemiluminescence can also occur when an excited species produced by a chemical reaction transfers energy to another species and luminesces. This analytical technique is also highly sensitive and selective. The detection limits are dependent on reagent purity, and, consequently, they lie between the parts-per-billion and the parts-per-million range.

Quantum dots are highly fluorescent and can be used in chemiluminescence reactions. Therefore, it is important to understand the luminescence process.

### Principle of Fluorescence

Fluorescence spectroscopy is one of the most popular analytical techniques used when characterizing quantum dots. Several factors contribute to its popularity. For instance, fluorescence spectrophotometers are highly sensitive due to the relationship between the source radiant power and the concentration of the solution. They are highly selective because only a relatively small number of molecules show significant luminescence. In addition, fluorometric methods provide wider linear dynamic ranges than absorption techniques. Finally, they have better detection limits, specifically one to three orders of magnitude better than absorption spectroscopy (56).

Quantum dots have the ability to emit radiation after it has absorbed radiation. This process is often referred to as luminescence. Luminescence includes fluorescence and phosphorescence. The best method of understanding the luminescence process is via a Jablonski diagram, which is shown in Figure 1 (56).

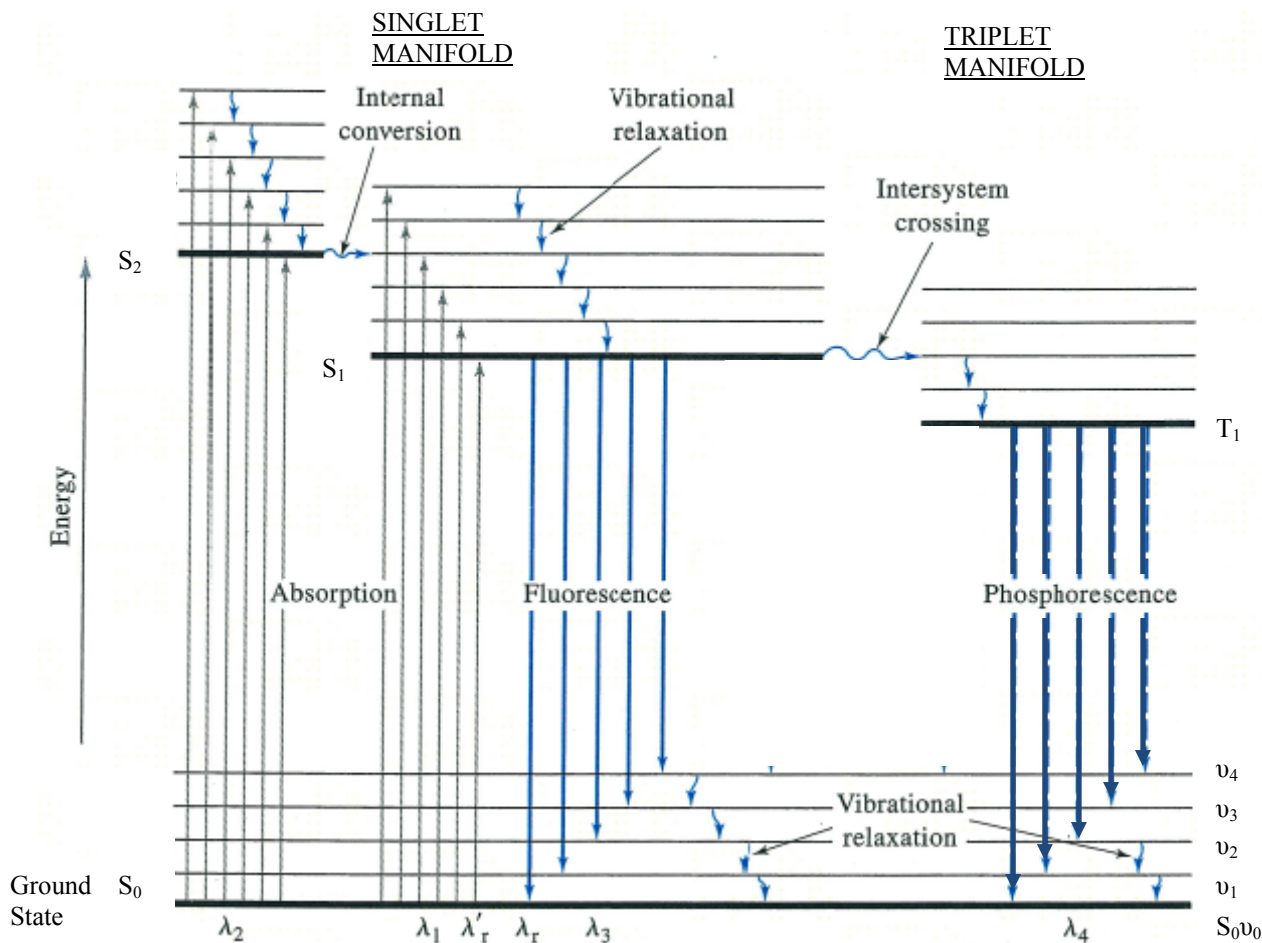


Figure 1. A simplified Jablonski diagram showing the various electronic and vibronic levels and the processes possible

The electronic ground state of a fluorescent molecule is represented by the bold horizontal lines labeled  $S_0$ . The ground state is usually in a singlet state. The bold horizontal lines far above the ground state represent the second electronic singlet state ( $S_2$ ), the first electronic singlet state ( $S_1$ ), and the first electronic triplet state ( $T_1$ ), respectively (56).

While at room temperature, the fluorescent molecule exists in the various levels of ground vibrational states ( $v_n$ ), usually at the lowest ( $S_0v_0$ ). All of the electron spins are paired and of opposite spins. When excited by a photon of a given wavelength, one electron is

promoted to an allowed vibronic level of a singlet excited state, whether  $S_1$  or  $S_2$ . This takes place rapidly within  $10^{-15}$  to  $10^{-14}$  s (56).

As time elapses, the stability of the electron in the excited state decreases, and the electron returns to its ground state via several pathways. For example, vibrational relaxation takes place as energy is released by collisions with the solvent molecules. In addition, energy can be lost through other radiative or radiationless transitions. Through a radiationless transition, the electron can relax from the lower vibrational state of the higher electronic state ( $S_2$ ) to the higher vibrational state of the lower electronic state ( $S_1$ ). This is known as the internal conversion. Here, the excited states are of the same multiplicity. In addition, no energy is lost because as the crossover occurs the potential energies of the two excited states remain equal. Then, vibrational relaxation can occur again to bring it to its ground vibrational state ( $S_0$ ) and emit energy simultaneously through a process called fluorescence. The average lifetime of fluorescence is  $10^{-10}$  to  $10^{-5}$  s (56). The equation below demonstrates the relationship between the lifetime and the fluorescence intensity:

$$I = I_0 e^{-t/\tau} \quad [1]$$

$I$  represents the fluorescence intensity at time  $t$ .  $I_0$  represents the maximum intensity after excitation.  $t$  represents the time during relaxation.  $\tau$  represents the lifetime of the excited state (57).

The spin of the electron can change and cause the multiplicity of the fluorophore to change as well. When this occurs, the electron is changing from an excited singlet state ( $S_1$ ) to an excited triplet state ( $T_1$ ). This is known as intersystem crossing, and it competes with fluorescence. As the electron relaxes to its ground vibrational state ( $S_0$ ) from the triplet state, the

emission of radiation is known as phosphorescence. The average lifetime of phosphorescence is  $10^{-4}$  to seconds or longer. However, intersystem crossing is less probable because it involves a change in spin state, which is considered a forbidden transition due to quantum mechanical reasons (56).

### Principle of Chemiluminescence

Chemiluminescence occurs when a chemical reaction produces an electronically excited species that emits light as it returns to its ground electronic state. An example of this type of luminescence is luminol chemiluminescence, which is illustrated in the following equations:



where A is luminol and B is an oxidant, such as hydrogen peroxide. C and D represent products, and C\* represents an excited species of C.  $h\nu$  represents the emitted light of frequency  $\nu$ , and h is the Planck constant (56).

Chemiluminescence can also occur when an electronically excited species transfers energy to another species that luminesces. This phenomenon is demonstrated in peroxyoxalate chemiluminescence and is exemplified by bis(2,4,6-trichlorophenyl) oxalate (TCPO):



where F is the fluorophore that accepts that transferred energy from the excited species C\* (58).

The intensity of chemiluminescence is based upon the following equations:

$$I_{CL} = \phi_{CL} (d[C] / dt) \quad [7]$$

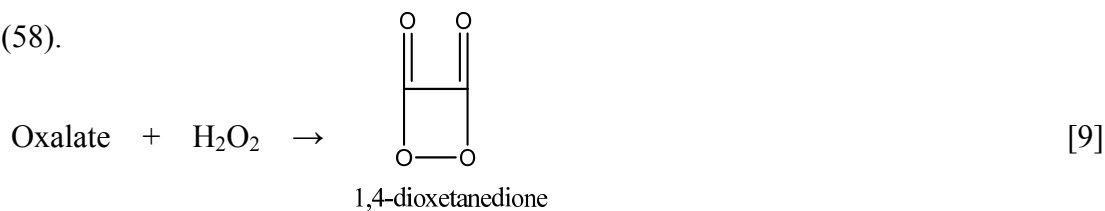
$$I_{CL} = \phi_{EX} \phi_{EM} (d[C] / dt) \quad [8]$$

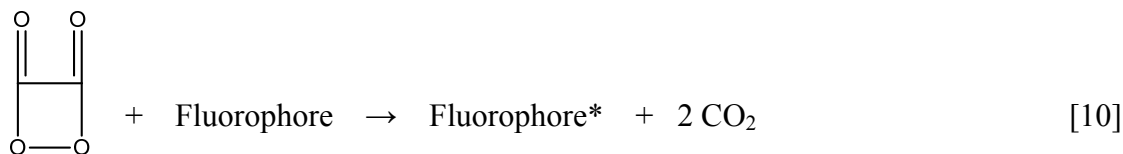
where  $I_{CL}$  is the radiant intensity (photons per unit time),  $\phi_{CL}$  is the chemiluminescence quantum yield (photons per molecule reacted),  $(d[C] / dt)$  is the rate of the chemical reaction, and  $\phi_{EX}$  and  $\phi_{EM}$  are the excitation and emission quantum yields, respectively. The chemiluminescence intensity decreases as the reagent is consumed over time (56).

Chemiluminescence is becoming more popular for several reasons. For instance, it is highly selective and sensitive. In addition, the simplicity of the instrumentation requires only a reaction vessel and a photomultiplier tube. No wavelength selector is needed because the radiation comes from the reaction between the reagent and the analyte. Because the detection limits are dependent upon reagent purity, the detection limits lie between the parts-per-billion and the parts-per-million range (56).

#### Peroxyoxalate Chemiluminescence

Rauhut and coworkers synthesized and characterized the chemiluminescent properties of peroxyoxalates (56). Oxalyl chloride was reacted with fluorescent organic compounds and hydrogen peroxide to produce chemiluminescence. The reaction between other oxalates, including oxalic anhydrides and substituted phenyloxalates, and hydrogen peroxide were also researched (60, 61). The mechanism for peroxyoxalate chemiluminescence is demonstrated below (58).





After the reaction between the peroxyoxalate compound and the hydrogen peroxide has occurred, the 1,4-dioxetanedione intermediate transfers its energy to the fluorophore. The fluorophore emits light as the excited species returns to its ground vibrational state (58). One of the most widely used reagents is TCPO, shown in Figure 2.

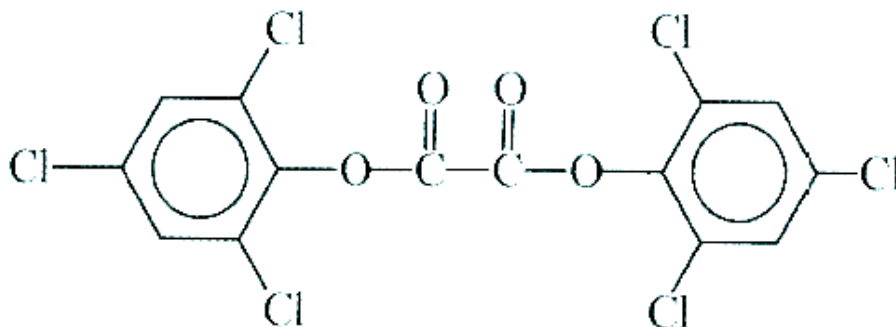


Figure 2. The chemical structure of bis(2,4,6-trichlorophenyl) oxalate, TCPO

Peroxyoxalate chemiluminescence is widely used for chemiluminescent analyses for several reasons. For example, peroxyoxalates, specifically TCPO, are easily synthesized and are highly stable over a wide pH range. The TCPO chemiluminescence has a wide linear dynamic range, four orders of magnitude of concentration or more. In addition, peroxyoxalate chemiluminescence can be applied to various types of analysis because different fluorophores can be used (62, 63).

## Applications of Peroxyoxalate Chemiluminescence

Peroxyoxalate chemiluminescence has been used in analyzing immobilized amino aromatics as fluorophores (64). In the chemiluminescence detection flow cell, Ponten and coworkers immobilized the amino aromatics on various glass bead surfaces. Imidazole was used to catalyze the hydrogen peroxide and TCPO reaction. The best fluorophore was 3-aminofluoranthene immobilized on controlled pore glass beads because the detection limit for hydrogen peroxide was 3 fmol (64).

Peroxyoxalate chemiluminescence has also been used to analyze glucose in urine (63). Williams and coworkers measured the hydrogen peroxide produced via enzyme catalysis of glucose. Glucose reacted with glucose oxidase in a buffer solution. The hydrogen peroxide produced proceeded to react with TCPO and perylene, which was the fluorophore. The linear dynamic range was from  $10^{-7}$  M to  $10^{-3}$  M hydrogen peroxide. Uric acid could have interfered with the chemiluminescent analysis. However, the buffer solution and the speed of the reaction prevented the interference, and an accurate analysis of glucose in urine samples was achieved (63).

## Research Proposal

When synthesizing CdSe quantum dots, most chemists use a colloidal synthesis procedure. It is a simple procedure, and large quantities of high-quality quantum dots are produced at minimal costs (50-52). According to previous research, the colloidal synthesis is more time-based (46, 54). In other words, the precursor is added to the mixture at one particular temperature, and aliquots of the solution are removed from the heat source at different times.

While this method is an efficient way of synthesizing CdSe quantum dots, only a small yield of a specific size can be produced at one time.

Therefore, this called for an attempt to investigate a synthetic procedure that would give a higher yield of CdSe quantum dots of various sizes and information concerning their luminescence properties. To achieve this, the following research proposal was used to guide the studies of the CdSe quantum dots and their luminescence properties:

- Investigate the synthesis of CdSe quantum dots via a temperature-based colloidal procedure.
- Investigate procedures to immobilize the CdSe quantum dots and the properties of the immobilized CdSe sol-gels.
- Investigate the luminescence properties via fluorescence and chemiluminescence of the sol-gel immobilized quantum dots and their figures of merit for possible applications.



## CHAPTER 3

### EXPERIMENTAL PROCEDURE

This chapter highlights the experimental procedures carried out to synthesize pure CdSe quantum dots and immobilized sol-gels and to establish their luminescence properties.

#### Reagents Used

All of the reagents used were of the highest purity available from commercial sources and were ACS certified. Therefore, no additional purification procedures were required.

1. 98 % Tetraethyl orthosilicate (TEOS) purchased from Acros Chemical Company (New Jersey)
2. 99 % Imidazole, 98 % oxalyl chloride, 99 % triethylamine, 90 % trioctylphosphine (TOP), and 98 % 2,4,6-trichlorophenol purchased from Aldrich Chemical Company (Milwaukee, WI)
3. 98.9 % Cadmium oxide, 99 % oleic acid, 99 % selenium powder, and 90 % 1-octadecene purchased from Alfa Aesar Chemical Company (Ward Hill, MA)
4. Acetonitrile, cyclohexane, 95 % ethanol, hydrochloric acid (HCl), and 30 % hydrogen peroxide (H<sub>2</sub>O<sub>2</sub>) purchased from Fisher Scientific (Pittsburgh, PA)
5. Deionized water acquired from US Filter Company (Pittsburgh, PA)

## Preparation of Stock Solutions

### Selenium Precursor Solution

Approximately 30 mg of Se powder was placed in a 25-mL flask. It was dissolved in 5.0 mL of 1-octadecene and 0.4 mL of TOP. The solution was heated to enhance the dissolving process. The solution was stored at room temperature.

### Imidazole Solution

Imidazole solution (100 mg/mL) was prepared by dissolving 1.0 g of imidazole in 10 mL of deionized water. The solution was stored in the refrigerator.

### Hydrogen Peroxide Solution

The H<sub>2</sub>O<sub>2</sub> solution ( $1.75 \times 10^{-1}$  M) was prepared by diluting 1 mL of 30 % H<sub>2</sub>O<sub>2</sub> in a 50-mL volumetric flask with deionized water. The solution was stored in the refrigerator.

## Synthesis of CdSe Quantum Dots

CdSe quantum dots were first synthesized by following the procedures described by Boatman, Lisensky, and Nordell (29). Approximately 13 mg of CdO was added to a 25-mL round-bottom flask. The CdO was dissolved in 10 mL of 1-octadecene and 0.6 mL of oleic acid. The solution was heated to 225 °C, and 1.0 mL of the Se precursor solution was added. Using a pipettor, 1.0 mL aliquots were removed every 10 seconds and placed in a test tube. As time elapsed, the color of the solution changed from yellow to red, and the size of the quantum dots increased. With this method, the color of the solution changed very rapidly, and, consequently, it was difficult to control the size of the quantum dots. Later the published procedure was modified and found to be just as satisfactory. This modified procedure is described below.

Approximately 13 mg of CdO was added to a 50-mL flask. The CdO was dissolved in 10 mL of 1-octadecene and 0.6 mL of oleic acid. Six different solutions were made and heated to the following temperatures: 125 °C, 160 °C, 195 °C, 210 °C, and 225 °C. Once the solution reaches the respective temperature, 1.0 mL of the Se precursor solution was added. The solution remained under the heat source for 15-20 seconds and was placed in a room temperature vial to prevent further growth of the quantum dots. This method was highly similar to a procedure performed by Shukla and Nigra (65). In that particular synthesis, various solvents of different boiling points were used. The Se precursor was added, and the solution was allowed to reflux. Quantum dots of different sizes were produced as solutions of different colors were obtained, as reported in the literature (29).

### Preparation of Working Solutions

#### Preparation of Quantum Dot Solutions for Linearity Studies

Exactly 20-, 50-, and 100- $\mu$ L aliquots of quantum dot solution were diluted in 5-mL volumetric flasks with cyclohexane. These samples were ready for fluorescent measurements.

#### Preparation of Quantum Dot Solutions for Obtaining an Emission Spectrum

Exactly 50- $\mu$ L aliquots of quantum dot solution were diluted in 5-mL volumetric flasks with cyclohexane. These samples were ready for fluorescent measurements.

#### Preparation of Quantum Dot Solutions for Immobilization Studies

The decanted liquid of quantum dots left over from immobilization process was diluted with 2.0 mL of cyclohexane. These samples were ready for fluorescent measurements.

### TCPO Solution

The TCPO solution (7.5 mg/mL) was prepared by dissolving 0.30 g in 40 mL of acetonitrile. The solution was sonicated for 1 hour.

### Preparation of Hydrogen Peroxide Solutions for Linearity Test

The calibrating solutions were prepared by diluting appropriate volumes of  $1.0 \times 10^{-1}$  M  $\text{H}_2\text{O}_2$  in separate 10-mL volumetric flasks. Thus, a  $1.75 \times 10^{-2}$  M  $\text{H}_2\text{O}_2$  solution was prepared by diluting 1.0 mL of  $1.75 \times 10^{-1}$  M  $\text{H}_2\text{O}_2$  with deionized water. Also,  $8.75 \times 10^{-3}$  M,  $3.50 \times 10^{-3}$  M,  $3.50 \times 10^{-4}$  M,  $8.75 \times 10^{-5}$  M, and  $3.75 \times 10^{-5}$  M  $\text{H}_2\text{O}_2$  solutions were prepared by diluting, respectively, 5.0 mL, 2.0 mL, 200  $\mu\text{L}$ , 50  $\mu\text{L}$ , and 21  $\mu\text{L}$  of  $1.75 \times 10^{-2}$  M  $\text{H}_2\text{O}_2$  in with deionized water. A  $1.75 \times 10^{-3}$  M  $\text{H}_2\text{O}_2$  solution was prepared by diluting 2.0 mL of  $8.75 \times 10^{-3}$  M  $\text{H}_2\text{O}_2$  with deionized water. An  $8.75 \times 10^{-4}$  M  $\text{H}_2\text{O}_2$  solution was prepared by diluting 5.0 mL of  $1.75 \times 10^{-3}$  M  $\text{H}_2\text{O}_2$  with deionized water. A  $1.75 \times 10^{-4}$  M  $\text{H}_2\text{O}_2$  solution was prepared by diluting 2.0 mL of  $8.75 \times 10^{-4}$  M  $\text{H}_2\text{O}_2$  with deionized water.

### Preparation of the Immobilized Quantum Dots

Approximately 0.5 g of chromosorb, glass bead, silica gel, and alumina were placed in separate 10-mL beakers. Exactly 1.0 mL of quantum dot solution was added. The mixture was sonicated for 1 hr.

### Preparation of the Sol-Gels and Immobilization of Quantum Dots

The sol-gels were prepared by following the procedures described by Qingwen et al (66). Approximately 2.0 mL of TEOS, 0.5 mL of 95 % ethanol, and 25  $\mu\text{L}$  of 0.05 M HCl were mixed together in a 10-mL flask. After stirring, 0.5 mL of deionized water was added to the solution,

and the solution was sonicated for 30 minutes. Next, the immobilization of the quantum dots was carried out. For this, 0.8 mL of the quantum dot solution was added and stirred. The solution was placed in a plastic container and covered with parafilm. The parafilm was punctured multiple times with a small needle to facilitate the evaporation of the solvent slowly. The container was refrigerated at 4 °C for 3 weeks and sat in a room-temperature environment for 1 week.

### Preparation of TCPO

TCPO was prepared by following the procedures of Mohan and Turro (58). Approximately 25 mL of triethylamine was added to a 50-mL round-bottom flask. A distillation procedure was done to obtain 20 mL of distilled triethylamine, and it was cooled to 10 °C. An estimated 300 mL of benzene was dried using magnesium sulfate, and after 1 hour, 250 mL of the benzene was decanted. Exactly 19.8 g of 2,4,6-trichlorophenol was dissolved in 250 mL of the benzene and was cooled to 10 °C. Exactly 14 mL of the distilled triethylamine was added to the mixture, and 5.0 mL of oxalyl chloride was added dropwise while in a dark room. The solution was refrigerated for 24 hours. The treatment of the precipitate produced was modified somewhat. The precipitate was filtered and washed with benzene and petroleum ether. After drying via suction filtration, the white crystals of TCPO were placed in an amber glass bottle where they were not exposed to light.

### Procedure of Measurement

#### Optimization of Imidazole Study

Exactly 40-, 50-, 60-, and 80- $\mu$ L aliquots of imidazole solution were placed in 4 separate test tubes. After adding the imidazole, 3.0 mL of the TCPO solution was placed in the test tubes.

A single sol-gel with immobilized quantum dots was added to the test tube. Exactly 1.0 mL of  $8.75 \times 10^{-3}$  M  $\text{H}_2\text{O}_2$  was added to the test tubes. These samples were ready for chemiluminescent measurements.

### Reproducibility Studies

Exactly 50  $\mu\text{L}$  of imidazole solution and 3.0 mL of the TCPO solution were added to different test tubes. A single sol-gel with immobilized quantum dots was added to the test tube. Then, exactly 1.0 mL of  $8.75 \times 10^{-4}$  M  $\text{H}_2\text{O}_2$  was added to each of the test tubes for chemiluminescent measurements.

### Linearity Study Using One Sol-Gel

Exactly 50  $\mu\text{L}$  of imidazole solution and 3.0 mL of the TCPO solution were added to different test tubes. A single sol-gel with immobilized quantum dots was added to the test tube. For chemiluminescent measurements, exactly 1.0 mL of the following  $\text{H}_2\text{O}_2$  solutions:  $1.75 \times 10^{-4}$  M,  $8.75 \times 10^{-4}$  M,  $1.75 \times 10^{-3}$  M,  $8.75 \times 10^{-3}$  M, and  $1.75 \times 10^{-2}$  M was added to the separate test tubes.

### Linearity Study Using Multiple Sol-Gels

Exactly 50  $\mu\text{L}$  of imidazole solution and 3.0 mL of the TCPO solution were added to different test tubes. Three sol-gels with immobilized quantum dots were added to the test tube. For chemiluminescent measurements, exactly 1.0 mL of the following  $\text{H}_2\text{O}_2$  solutions:  $1.75 \times 10^{-4}$  M,  $8.75 \times 10^{-4}$  M,  $1.75 \times 10^{-3}$  M,  $8.75 \times 10^{-3}$  M, and  $1.75 \times 10^{-2}$  M was added to the separate test tubes.

### Linearity Study Using Crushed Sol-Gels

Exactly 50  $\mu\text{L}$  of imidazole solution and 3.0 mL of the TCPO solution were added to different test tubes. Two sol-gels with immobilized quantum dots were crushed and placed in the test tube. For chemiluminescent measurements, exactly 1.0 mL of the following  $\text{H}_2\text{O}_2$  solutions:  $3.75 \times 10^{-5}$  M,  $8.75 \times 10^{-5}$  M,  $1.75 \times 10^{-4}$  M,  $3.50 \times 10^{-4}$  M,  $1.75 \times 10^{-3}$  M, and  $3.50 \times 10^{-3}$  M was added to the separate test tubes.

### Instrumentation

#### Instrumentation for Fluorescence

The fluorescent signals were monitored by the Perkin-Elmer 650-10s Fluorescence Spectrophotometer. In this instrument, a 150 W xenon lamp was the radiation source, and a photomultiplier tube was used as the detector. The sensitivity was set at 1 and both the excitation and the emission slits were set at 2 nm. An excitation wavelength of 400 nm was used for all emission samples measurements. The samples were placed in a quartz cuvette. A schematic of the instrumentation is shown in Figure 3.

#### Instrumentation for Chemiluminescence

The chemiluminescent signals were measured by instrumentation assembled together in the laboratory. The Hamamatsu R928 photomultiplier tube was a detector, and the American Instrument Company microphotometer (Silver Spring, MD) was used to monitor the signals. They were recorded on the Model 680 Hewlett-Packard, Strip chart recorder. The percent full scale was set on 0.3, and the slit was opened to its maximum width. The samples were placed in micro test tubes. A representation of the instrumentation is shown in Figure 4.

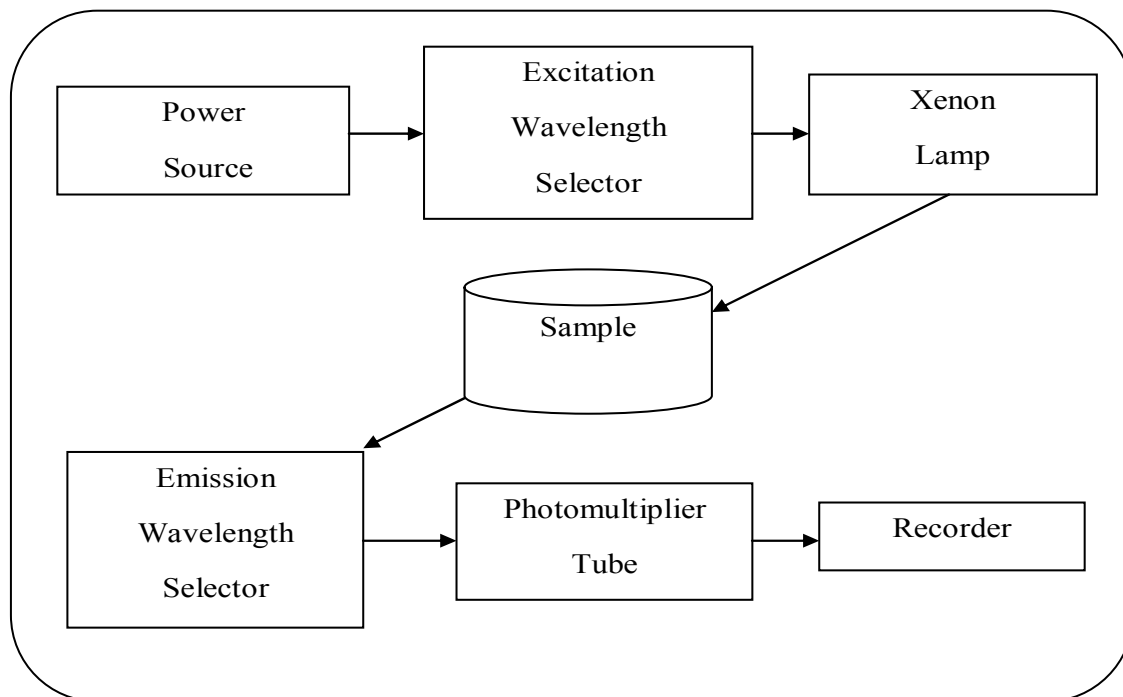


Figure 3. Schematic diagram of the fluorescence spectrophotometer

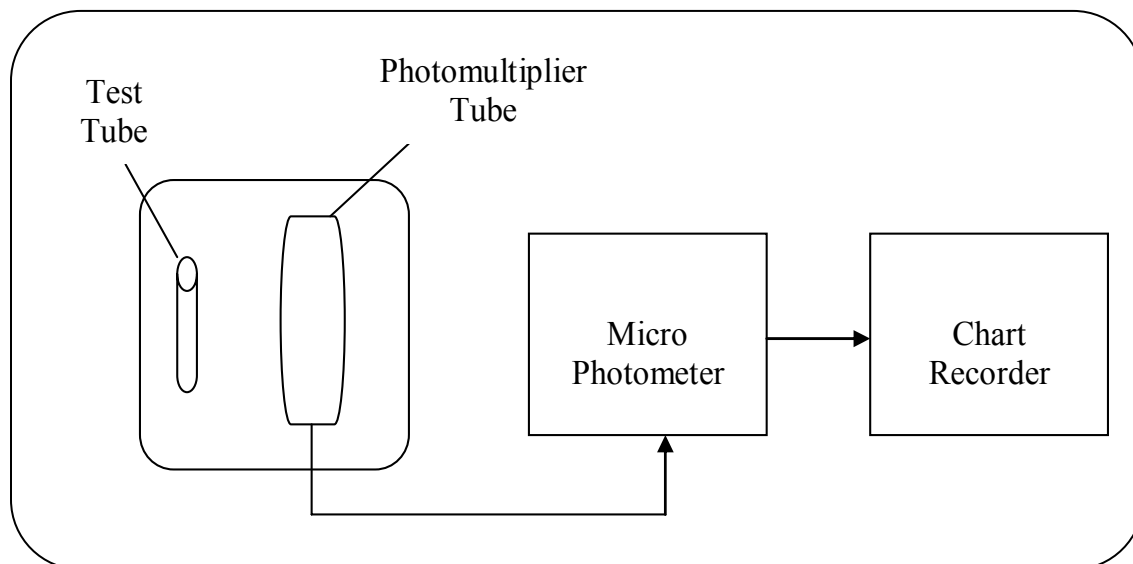


Figure 4. Schematic diagram of the chemiluminescent instrumentation



## CHAPTER 4

### RESULTS AND DISCUSSION

The results of all the fluorescence and chemiluminescence experiments are presented and discussed in this chapter. The results were used to verify that the synthesis, immobilization of the CdSe quantum dots, and the stated objectives were successfully achieved.

#### Fluorescence Studies of the Quantum Dot (QD) Solutions

##### Time-Based QD Synthesis

The time-based quantum dot synthesis was performed according to the procedure (29) previously stated. In this procedure, quantum dots of different sizes were obtained by how long the reaction was allowed to proceed and to remove needed amounts of the quantum dots of given sizes at regular time intervals. Various sizes of quantum dots were thus synthesized, and they emitted light ranging from the yellow to the red end of the visible spectrum. However, only a small volume of the different sized quantum dots were obtained by this method of synthesis. By the time the first 1.0-mL aliquot was removed, the entire reaction solution had turned red, producing the larger sized quantum dots. The time intervals between the removals of different size quantum dots produced were quite small, and one needed to be quick and efficient in carrying out this procedure. This method was therefore inconvenient, and much of the yield was not satisfactory. Therefore, a temperature-based procedure was tried and performed.

##### Temperature-Based QD Synthesis

The proposed method for synthesizing the quantum dots of different sizes was a temperature-based synthesis. In this procedure, one of the reagents was heated to different

temperatures before the other precursor was added. The reaction was then allowed to proceed to completion. This procedure proved to be just as satisfactory as the time-based synthesis. The size of the quantum dots was better controlled by heating the Cd precursor solution to a particular temperature and then adding the Se precursor solution to it. The reaction was then allowed to proceed for 15-20 seconds. The larger quantum dots were obtained at higher temperatures and vice versa for the smaller quantum dots. The larger quantum dots grew at a quicker rate at higher temperatures. The quantum dots obtained in this manner emitted light ranging from the yellow to red end of the visible spectrum as well. In addition, a greater yield of the quantum dots was obtained. This method was later found to be quite similar to a procedure performed by Shukla and Nigra (65). In that particular synthesis, various solvents at different boiling points were used. The Se precursor was added, and the solution was allowed to reflux. Quantum dots of different sizes were produced. They performed various analyses to verify the synthesis of the quantum dots of different sizes and to examine their luminescence properties.

#### Effect of QD Size on the Emission of Light

The Se precursor was added to the Cd precursor after the Cd precursor had reached the following temperatures: 125 °C, 160 °C, 195 °C, 210 °C, and 225 °C. After adding the Se precursor, the reaction was allowed to proceed to completion for 15-20 seconds. The actual size of the quantum dots could have been measured by using a transmission electron microscope or a scanning electron microscope, but neither microscope was available in the laboratory. However, from the color of the quantum dot suspensions obtained and from their emission spectra, the quantum dots were definitely of different sizes and progressed from a smaller size to a larger size with an increase in temperature. Shukla and Nigra (65) also found that the larger quantum dots were obtained at higher temperatures and at lower temperatures for the smaller quantum dots.

The quantum dots were suspended in the solvent 1-octadecene, and solutions of various colors were obtained. When exposed to ultraviolet light, the quantum dots emitted different wavelengths of light. Table 1 shows the color of the solutions when the reaction reached completion at the specific temperature, and it also tabulates the colors of light emitted when exposed to ultraviolet light.

Table 1. Color of CdSe QD Solutions Synthesized by Heating Cd and Se Precursors to Different Temperatures and When Exposed to Ultraviolet Light

Temperature (°C)	Color (Visually to the Eyes)	Color (Under Ultraviolet Light)
125	Yellow	Blue
160	Dark Yellow	Dark Green
195	Orange	Green
210	Dark Orange	Dark Yellow
225	Red	Yellow

The color of the quantum dot solutions visually ranged from yellow to red. When exposed to ultraviolet light, the quantum dots luminesced from blue to red. According to Boatman, et al. (29), larger quantum dots emit longer wavelengths of light, and shorter wavelengths are emitted for quantum dots of smaller sizes. Therefore, a red color is seen and yellow emission noted with large quantum dots, which form at higher temperatures in the new procedure.

#### Emission Spectra of QD

The fluorescence spectra of the different quantum dot solutions were obtained. The fluorescence spectra were obtained by varying the emission wavelengths while the excitation

wavelength remained at 400 nm. The fluorescence intensity was measured for emission monochromator setting ranging from 480 nm to 590 nm at 5 nm intervals. A plot of such a fluorescence emission spectrum for quantum dots synthesized at 210 °C is shown in Figure 5.

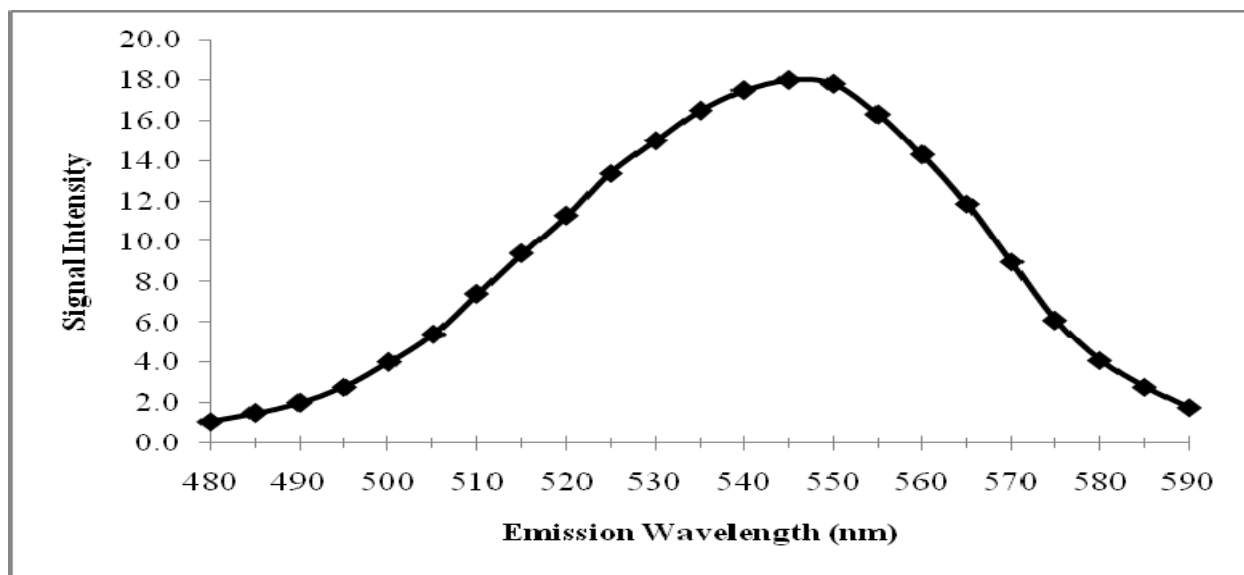


Figure 5. Plot of the fluorescence spectrum of QD synthesized at 210 °C ranging from 480 nm to 590 nm at 5 nm intervals. The excitation wavelength was set at 400 nm. The fluorescence intensity is given in arbitrary units.

This procedure was repeated with all of the CdSe quantum dot solutions produced at the five different temperatures. All of the measurements produced fluorescence spectra similar to that of Figure 5. When measuring the fluorescence of the quantum dot solutions of different sizes, the maximum intensity was observed at different emission wavelengths. These results are shown in Table 2.

The fluorescence intensity for the larger quantum dots was observed at longer wavelengths as expected. The emission spectrum was similar to that of the spectrum obtained by Shukla and Nigra, where the larger-sized quantum dots luminesced at longer wavelengths and

Table 2. Result of Maximum Emission Wavelength Peak with Varying Temperatures

Temperature (°C)	Maximum Wavelength Peak (nm)
125	455
160	505
195	525
210	550
225	575

vice versa (65). An attempt was made to carry out the synthesis at lower temperatures to obtain quantum dots of much smaller sizes, which might luminesce at shorter wavelengths. However, this attempt was not successful. It seems that a minimum temperature was needed to get the synthesis of quantum dots going at all.

#### Linearity Studies of Fluorescence Signal with Concentration of QD

The Perkin-Elmer 650-10s Fluorescence Spectrophotometer was used to measure the fluorescence intensity of the quantum dots of varying concentrations. A given size quantum dot solution was chosen for this study. A set of solutions of different concentrations for a given size quantum dot solution were prepared as previously stated, and the fluorescence intensity was measured. The quantum dot solution chosen was the one prepared at 195 °C. The results of this study are shown in Table 3.

These results were used to plot a calibration curve; the linear plot is shown in Figure 6. As seen in the plot, the fluorescence intensity of the chosen quantum dots was proportional to its concentration. The results showed a good linear dynamic range with a regression coefficient of

Table 3. Measurement of CdSe Quantum Dot Solution Fluorescence Prepared at 195 °C for Linearity Study with an Excitation and Emission Wavelengths of 400 nm and 535 nm, Respectively. The quantum dots were dissolved in cyclohexane in 5-mL volumetric flasks.

Volume of Quantum Dot Solution (μL)	Fluorescence Intensity
20	4.1
50	9.6
100	21.9

0.994. This procedure was repeated with the quantum dots of various sizes. All of the results in the same dynamic range were linear.

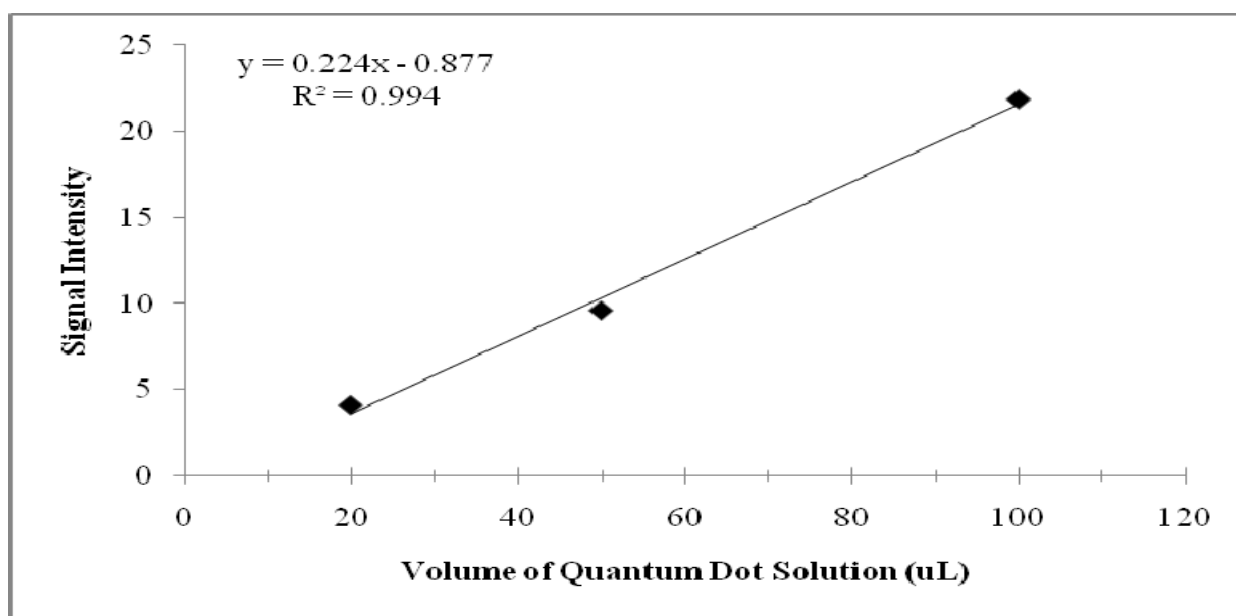


Figure 6. Plot of the fluorescence intensity of 195 °C QD solution dissolved in cyclohexane in 5-mL volumetric flasks. The excitation and emission wavelengths were 400 nm and 535 nm, respectively.

#### QD Immobilization by Adsorption Studies

A set of studies was conducted to see if the quantum dots could be easily immobilized on some solid supports. For these studies, the quantum dots synthesized at 160 °C and 195 °C were

used. The fluorescence spectrum of the quantum dots synthesized at 160 °C is shown in Figure 7.

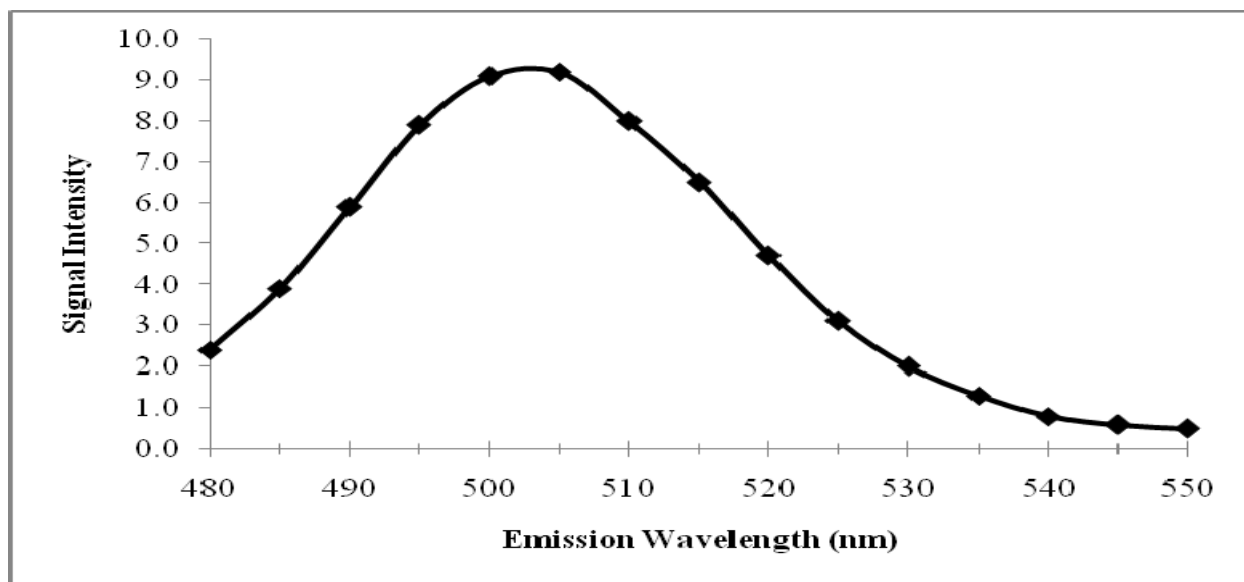


Figure 7. Plot of the fluorescence spectrum of QD synthesized at 160 °C ranging from 480 nm to 550 nm at 5 nm intervals. The excitation wavelength was set at 400 nm.

According to the procedures described in Chapter 3, the CdSe quantum dots were immobilized by adsorption on the following surfaces: chromosorb, glass bead, silica gel, and alumina. The 160 °C and 195 °C quantum dot solutions were chosen for this experiment. As the solutions were sonicated for 1 hr, some of the quantum dots adsorbed and remained bound to each surface. The fluorescence of the immobilized substances in the solid phase was measured. The plots for the immobilized chromosorb and glass bead are shown in Figure 8.

The quantum dot solution was decanted from the mixture after sonication. The decanted solutions were diluted with 2.0 mL of cyclohexane, and the fluorescence was measured. The plots for these results are shown in Figure 9.

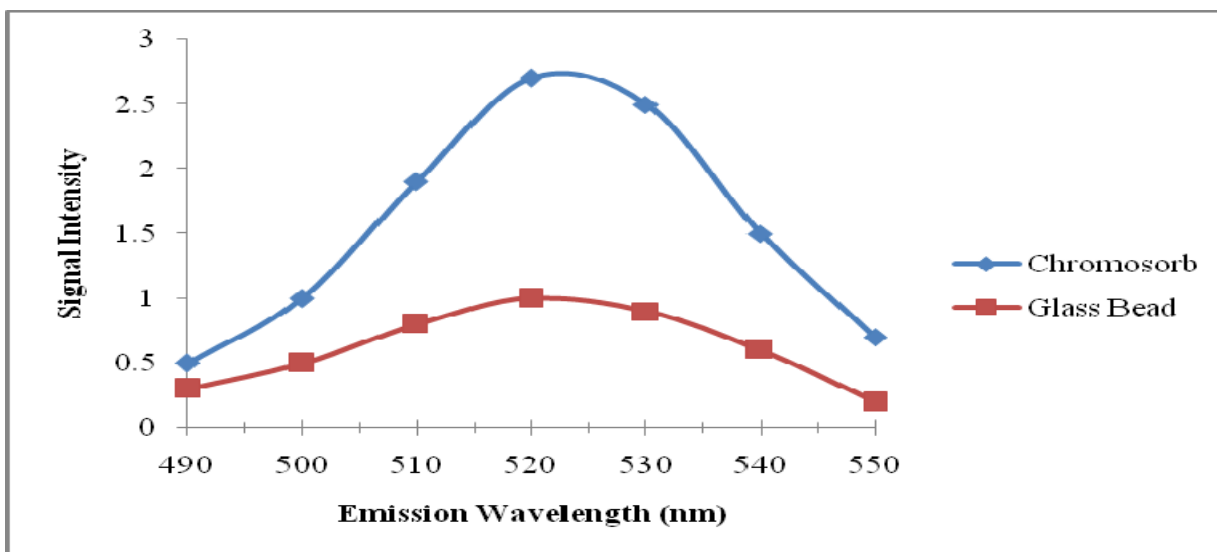


Figure 8. Plot of the fluorescence spectrum of immobilized 195 °C QD chromosorb and glass bead solids. The excitation wavelength was 400 nm, and the emission wavelength ranged from 490 nm to 550 nm.

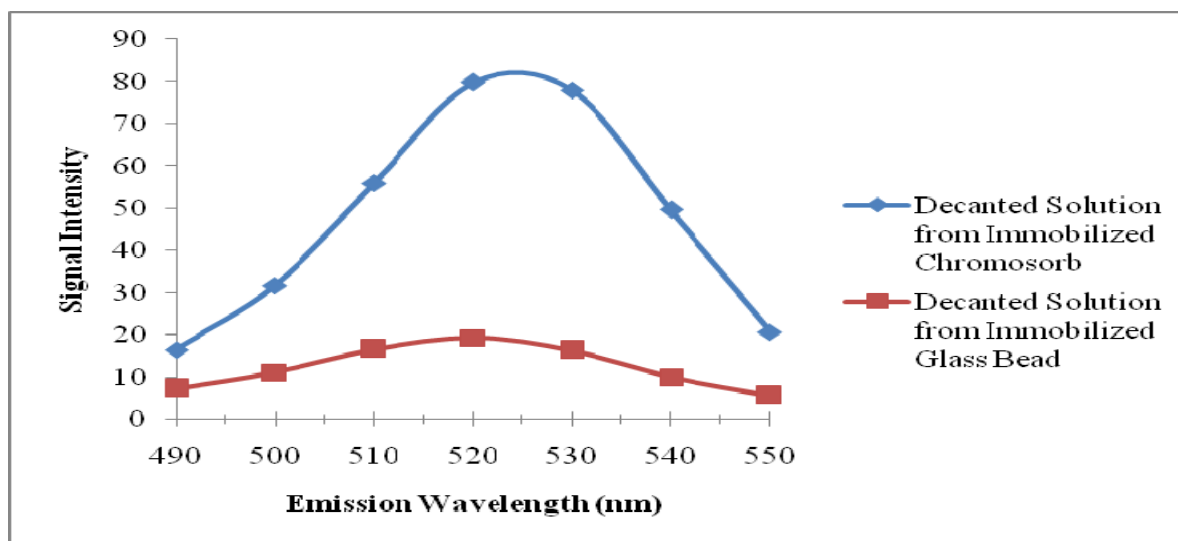


Figure 9. Plot of the fluorescence spectrum of 195 °C decanted QD solution from immobilized chromosorb and glass bead solids. The decanted solutions were diluted with 2.0 mL of cyclohexane. The excitation wavelength was 400 nm, and the emission wavelength ranged from 490 nm to 550 nm.

As seen in the plots, a high concentration of quantum dots remained in solution after adsorption. From Figures 8 and 9, the fluorescence intensity was much greater for the decanted



solutions than for the immobilized chromosorb and glass bead solids. There seemed to be a small shift in maximum emission wavelength for both the decanted solutions and the immobilized solid materials.

After examining these results, it can be concluded that the quantum dots were immobilized on chromosorb and glass bead only to a small extent. Very little of the quantum dot solution was immobilized on the chromosorb and glass bead surfaces more likely due to the polarity differences. The chromosorb and glass bead surfaces are more polar than the quantum dot solutions. Some soluble quantum dots were adsorbed on the surfaces. However, the amount adsorbed was not enough for use in practical analysis.

Similar experiments were also performed using silica gel and alumina. The fluorescence intensities for the immobilized silica gel and alumina were obtained and are plotted in Figure 10.

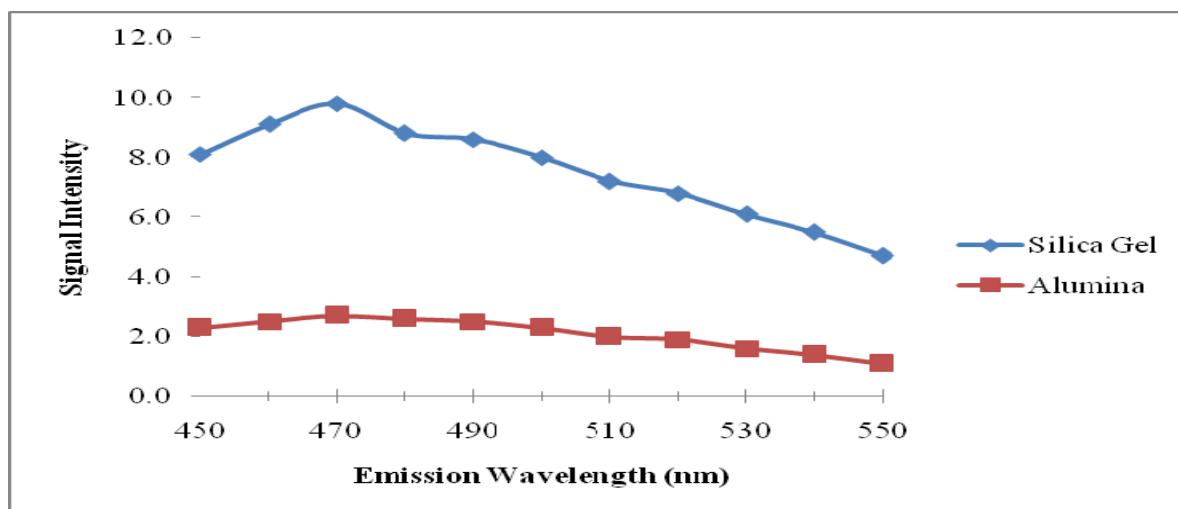


Figure 10. Plot of the fluorescence spectrum of immobilized 160 °C QD silica gel and alumina solids. The excitation wavelength was 400 nm, and the emission wavelength ranged from 450 nm to 550 nm.

The size of the quantum dots used for these experiments was smaller than those immobilized on the chromosorb and glass bead surfaces. It seems that more of the quantum dots

bound to the surface of the silica gel than any other surface. The fluorescence intensity for the silica gel solid was at least three times greater than the fluorescence intensities obtained on the other surfaces.

The remainder of the quantum dots left in solution after adsorption was decanted, diluted with 2.0 mL of cyclohexane, and the fluorescence was measured. The plots for these results are shown in Figure 11.

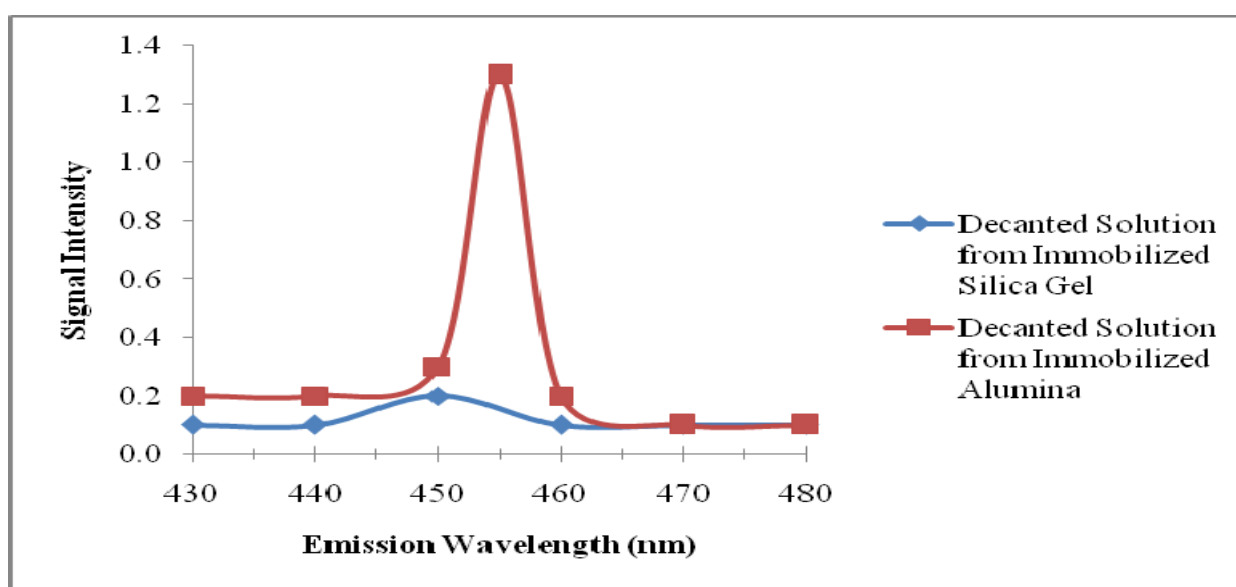


Figure 11. Plot of the fluorescence spectrum of 160 °C decanted QD solution from immobilized silica gel and alumina solids. The decanted solutions were diluted with 2.0 mL of cyclohexane. The excitation wavelength was 400 nm, and the emission wavelength ranged from 430 nm to 550 nm.

The fluorescence intensity for the decanted quantum dot solution was lower than that of the quantum dots adsorbed onto silica gel and alumina. These results are opposite of those observed for glass beads and chromosorb. In addition, the fluorescence spectrum obtained for the decanted quantum dot solution is much sharper and not as broad. It seems that by immersing the quantum dot solution in silica gel, quantum dots of certain size distribution are adsorbed onto

the silica gel, leaving a narrow quantum dot size distribution in the solution. Another interesting observation is that not only is the fluorescence spectrum much narrower, the peak maximum is also blue shifted to 455 nm from 505 nm in the original solution. This, however, is not the case for alumina.

The 160 °C quantum dot solution was also immobilized by using alumina of different mesh sizes. The mesh sizes of alumina used in the experiment were 100-150 mesh and 150-200 mesh. After sonicating the solutions for 1 hr, the quantum dots left in solution after adsorption were decanted and diluted with 2.0 mL of cyclohexane. The fluorescence of the decanted solutions was measured with an excitation monochromator setting of 400 nm and emission setting from 480 nm to 550 nm. The plots of the results are shown in Figure 12. The fluorescence intensities of the decanted solutions were compared.

As seen in Figure 12, the fluorescence intensity was smaller for the decanted solution from the 150-200 mesh alumina than for the 100-150 mesh alumina. More quantum dots were adsorbed on the alumina of 150-200 mesh. The larger the mesh number, the smaller the particle size. Therefore, the quantum dots remain bound to the alumina of a smaller particle size. More fine particles are present with a smaller particle size. More quantum dots compete for the same surface area with larger particles. However, smaller particles have larger surface areas, and, thus, more quantum dot particles can adsorb on the surface.

In addition, the fluorescence spectrum does not show the narrowing and blue-shift as seen with silica gel. But overall, immobilization by adsorption onto solid substrates does not seem to be desirable even though it is feasible.

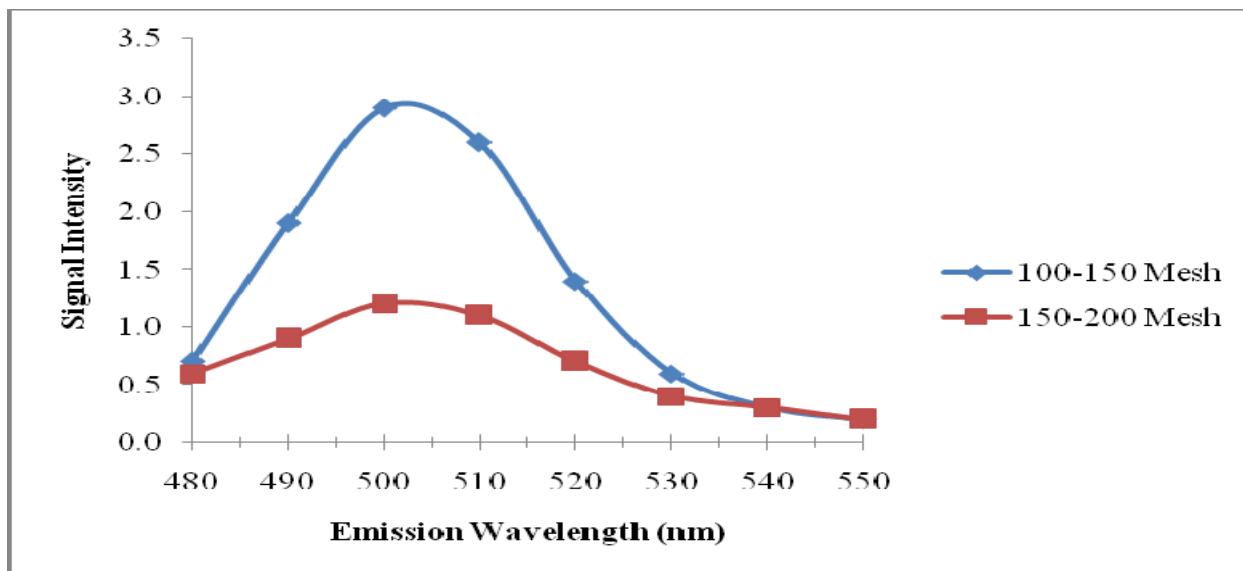


Figure 12. Plot of the fluorescence spectrum of 160 °C decanted QD solution from immobilized alumina with mesh sizes of 100-150 mesh and 150-200 mesh. The decanted solutions were diluted with 2.0 mL of cyclohexane. The excitation wavelength was 400 nm, and the emission wavelength ranged from 490 nm to 550 nm.

#### Feasibility Studies of Sol-Gel Immobilized QD in TCPO-CL

Peroxyoxalate chemiluminescence (CL) occurs when an electronically excited species transfers energy to another species that luminesces. The TCPO reacts with hydrogen peroxide in the presence of a catalyst to produce an energetic species, and energy from it is transferred to a fluorophore.

Chemiluminescence is becoming more popular for several reasons. For instance, it is highly selective and sensitive. In addition, the simplicity of the instrumentation requires only a reaction vessel and a photomultiplier tube. No wavelength selector is needed because the radiation comes from the reaction between the reagent and the analyte. Because the detection limits are dependent upon reagent purity, the detection limits lie between the parts-per-billion and the parts-per-million range (56).

Quantum dots were immobilized in sol-gels. These immobilized quantum dot sol-gels were studied to ascertain their feasibility as reusable fluorophore in TCPO-CL analysis. Immobilized sol-gel fluorophores were synthesized using the 210 °C quantum dot solution. The sol-gel with immobilized quantum dots was evaluated for use in TCPO-CL studies: optimization of imidazole, reproducibility studies, and linearity studies.

#### Optimization of Amount of Imidazole Catalyst

Imidazole, a base, was used as a catalyst for the TCPO-hydrogen peroxide CL reaction. Different volumes of imidazole were used to determine the optimum concentration to obtain the highest CL signal. As previously stated, 3.0 mL of the TCPO solution (7.5 mg/mL) was placed in different test tubes with the varying volumes of imidazole and a single sol-gel with immobilized quantum dots. Then, 1.0 mL of  $8.75 \times 10^{-3}$  M H<sub>2</sub>O<sub>2</sub> was added to each test tube, and the CL intensity was measured. The instrumentation assembled in the laboratory was used to obtain the CL results shown in Table 4. These results are also plotted in Figure 13.

Table 4. Results of the Optimization of Imidazole for TCPO-Hydrogen Peroxide CL Reaction

Imidazole (μL)	40	50	60	80
Signal Intensity	0.090	0.119	0.085	0.060

The results showed that the CL intensity increased as the volume of imidazole increased up to an optimum amount. Beyond this, the CL intensity began to decrease. The maximum CL intensity was obtained when 50 μL of the stock imidazole solution was added. Based upon these

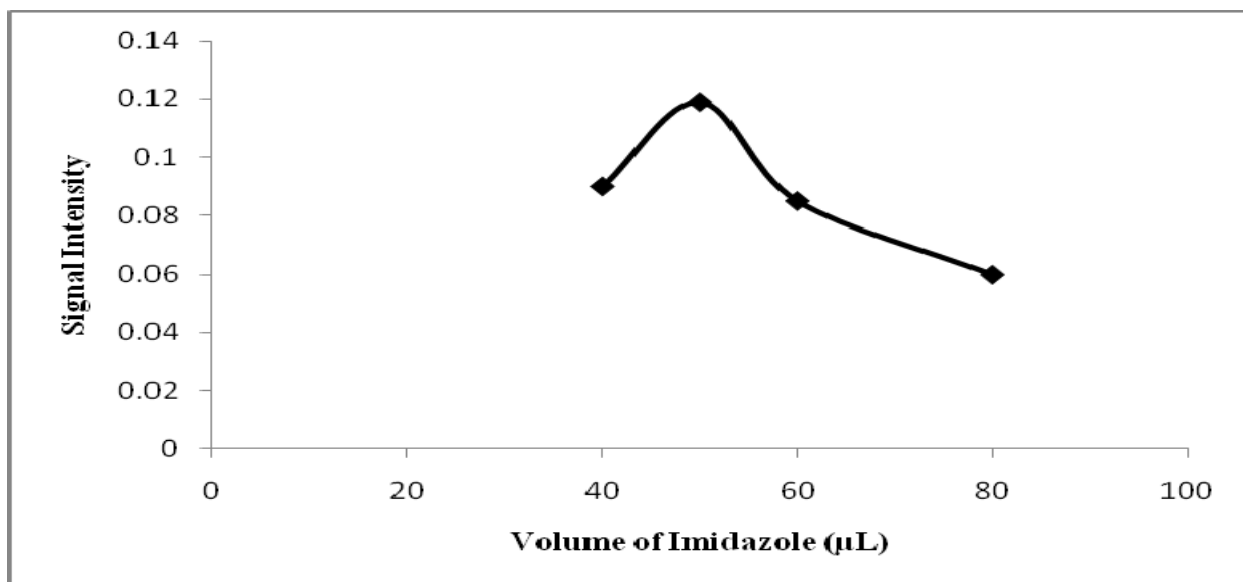


Figure 13. Plot of the results of the optimization of imidazole experiment for the TCPO (7.5 mg/mL) - hydrogen peroxide ( $8.75 \times 10^{-3}$  M) reaction. The concentration of the stock imidazole solution was 100 mg/mL. The CL intensity is given in arbitrary units.

results, 50 µL of the 100 mg/mL stock imidazole solution was used in all of the TCPO-CL reactions.

### Reproducibility Studies

An analytical method must be reproducible to be applicable for analysis with confidence. The method has to have high precision. To establish the reproducibility of the CL method, two experiments were performed. In the first experiment, five different  $8.75 \times 10^{-4}$  M  $H_2O_2$  solutions were prepared in separate 10-mL volumetric flasks. The CL intensity was measured by reacting 3.0 mL of TCPO and 50 µL of stock imidazole with the hydrogen peroxide solutions. The same single sol-gel with immobilized quantum dots was used in this experiment. Triplicate measurements of each hydrogen peroxide solution were obtained, and the mean and RSD for each solution were calculated. The results of the experiment are shown in Table 5.

Table 5. Results of Reproducibility Study of Proposed CL Method Using Five Different  $8.75 \times 10^{-4}$  M Hydrogen Peroxide Solutions

Trial	1	2	3	4	5
CL Intensity 1	0.0295	0.0239	0.0232	0.0282	0.0242
CL Intensity 2	0.0280	0.0220	0.0249	0.0211	0.0261
CL Intensity 3	0.0280	0.0261	0.0219	0.0280	0.0225
Mean	0.0285	0.0240	0.0233	0.0258	0.0243
RSD (%)	3.04	8.55	6.45	15.69	7.42
Total Mean	0.0252				
RSD (%)	10.86				

The precision of the data obtained for the five different hydrogen peroxide solutions are all less than an RSD of 10 % except for the fourth set. The combined mean of the 15 CL measurements was 0.0252, with an RSD of 10.86 %. The results demonstrated that the precision of the analytical method was satisfactory. The preparation of the different hydrogen peroxide solutions were quite precise because the RSD value, for the most part, was less than 10 %. It also showed that the sol-gel with immobilized quantum dots could be used multiple times without causing a significant change in results.

The second experiment involved using only a single preparation of  $8.75 \times 10^{-4}$  M  $H_2O_2$  solution. Exactly 3.0 mL of TCPO and 50  $\mu$ L of imidazole reacted with 1.0 mL of the hydrogen peroxide solution. This test was performed numerous times over several weeks using the same single sol-gel with immobilized quantum dots and newly prepared hydrogen peroxide solutions of the same concentration. The purpose of both this and the previous experiments was to examine the stability of the sol-gel with immobilized quantum dots. The results of this experiment are shown in Table 6.

Table 6. Results of Reproducibility Study of Proposed CL Method Using a Single Sol-Gel with Immobilized QD. Fixed volumes of TCPO (7.5 mg/mL) and Imidazole (100 mg/mL) reacted with 1.0 mL of  $8.75 \times 10^{-4}$  M Hydrogen Peroxide Solution.

Trial	1	2	3	4	5	6	7	8	9	10
CL	0.0209	0.0210	0.0192	0.0191	0.0184	0.0179	0.0227	0.0193	0.0155	0.0161
Trial	11	12	13	14	15	16	17	18	19	20
CL	0.0145	0.0143	0.0149	0.0136	0.0149	0.0130	0.0132	0.0129	0.0134	0.0137
Mean	0.0164									
RSD (%)	18.88									

From the data obtained, the mean was 0.164, with an RSD of 18.88 %. When combining all of the data above and subsequent ones, it was concluded that the same sol-gel with immobilized quantum dots could be used for analysis at least 45 times and still provide good results. This showed that the sol-gel with immobilized quantum dots remained stable and continued to luminesce over several weeks at a time. The CL intensity decreased slightly as more analyses were performed because some of the quantum dots might have been lost. This might be evidenced by noting that the sol-gel with immobilized quantum dots was losing some of the red color that was originally present before the analyses.

#### Linearity Studies of CL Intensity with H<sub>2</sub>O<sub>2</sub> Concentration Using Sol-Gel Immobilized QD

One Sol-Gel. Linearity studies were conducted by reacting TCPO with varying concentrations of hydrogen peroxide to produce CL using a single sol-gel with immobilized quantum dots as previously described. The hydrogen peroxide solution of a given concentration was prepared in triplicates separately. The duplicate CL measurement for each of the triplicate solutions were obtained. The results are shown in Table 7, where 1, 2, and 3 represent the triplicate preparations.



Table 7. Results of Linearity Studies of CL Intensity with Hydrogen Peroxide Using a Single Sol-Gel with Immobilized QD

H <sub>2</sub> O <sub>2</sub> (M)	1.75 x 10 <sup>-4</sup>	8.75 x 10 <sup>-4</sup>	1.75 x 10 <sup>-3</sup>	8.75 x 10 <sup>-3</sup>	1.75 x 10 <sup>-2</sup>
CL Intensity 1	0.0081	0.0191	0.0252	0.0538	0.0749
	0.0080	0.0183	0.0244	0.0551	0.0758
CL Intensity 2	0.0062	0.0181	0.0239	0.0551	0.0778
	0.0051	0.0185	0.0241	0.0582	0.0791
CL Intensity 3	0.0050	0.0172	0.0238	0.0571	0.0762
	0.0073	0.0160	0.0226	0.0535	0.0790
Mean	0.0066	0.0179	0.0240	0.0555	0.0771
RSD (%)	21.02	6.18	3.55	3.33	2.28

Because the experiment was repeated multiple times, the mean values and RSD values were calculated. The mean CL intensities with the corresponding hydrogen peroxide concentrations are plotted in Figure 14.

There was more variation in the CL intensities of the lower concentrations of hydrogen peroxide than with the higher concentrations. This is shown through the RSD values. The RSD value for the lowest concentration of hydrogen peroxide, 1.75 x 10<sup>-4</sup> M, was 21.02 % while all the others were less than 6.20 %. It was concluded that the detection limit was being approached. Therefore, the useful linearity range was from 8.75 x 10<sup>-4</sup> M to 1.75 x 10<sup>-2</sup> M H<sub>2</sub>O<sub>2</sub> solution. The linearity curve is shown in Figure 15. The CL intensity was proportional to the hydrogen peroxide concentration within this range of hydrogen peroxide concentration.

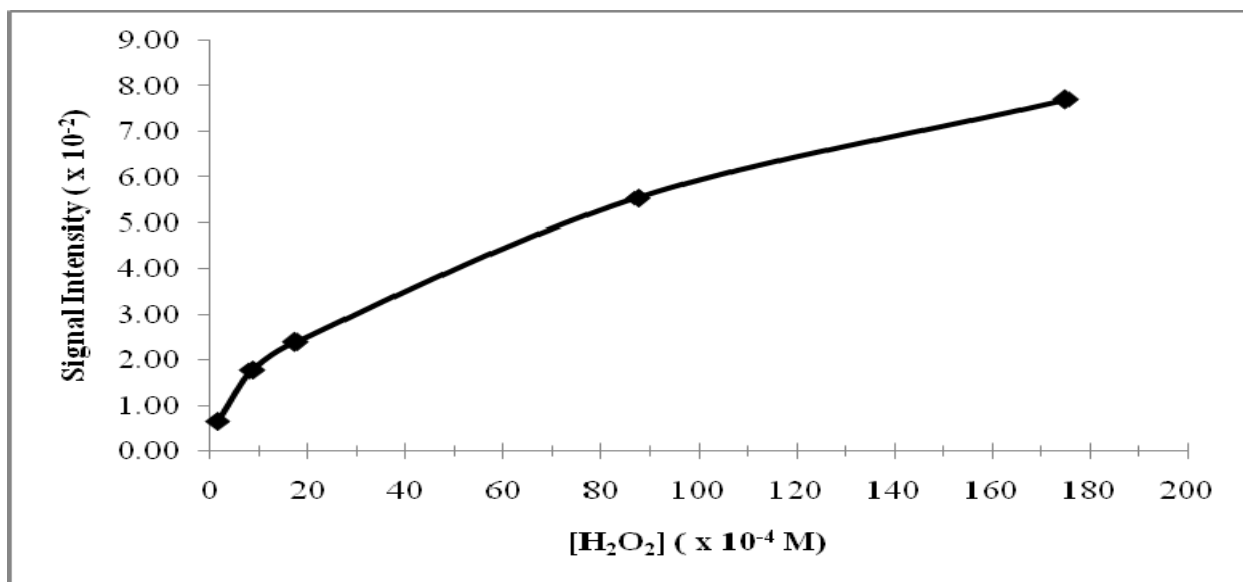


Figure 14. Plot of the average duplicate CL measurements on each separately prepared triplicate hydrogen peroxide solution using 3.0 mL of TCPO, 50  $\mu$ L of imidazole, and a single sol-gel with immobilized QD

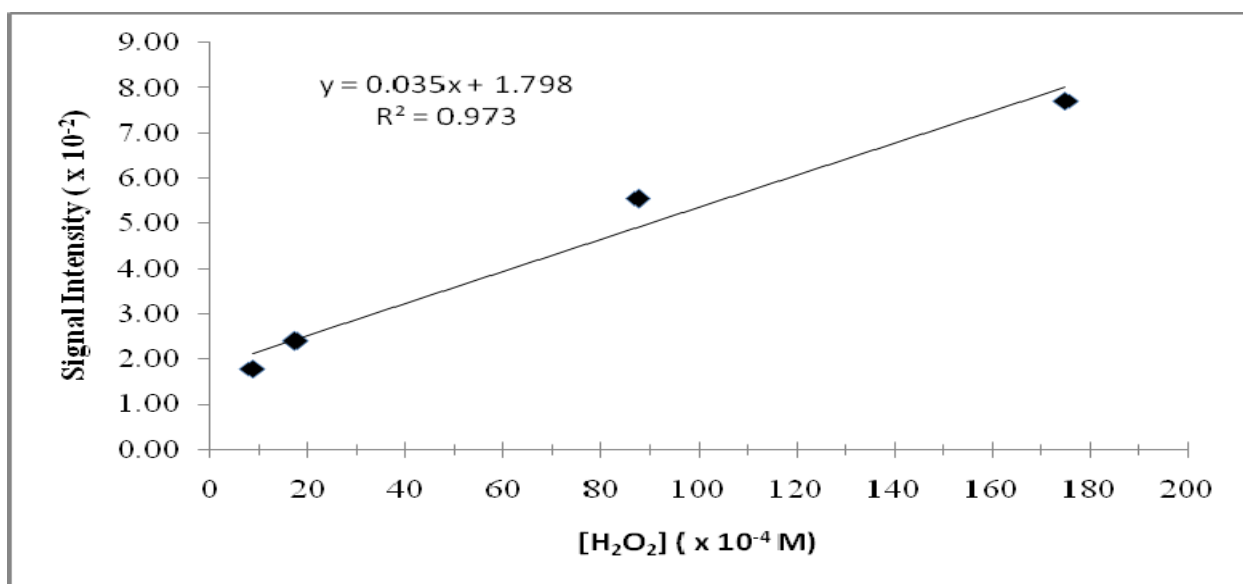


Figure 15. Plot of the linearity curve of the average duplicate CL measurements on each separately prepared triplicate hydrogen peroxide solution using 3.0 mL of TCPO, 50  $\mu$ L of imidazole, and a single sol-gel with immobilized QD

Multiple Sol-Gels. The purpose of this experiment was to see if a higher CL signal could be achieved with more quantum dots. The CL intensity was measured by reacting fixed volumes

of TCPO and imidazole with various concentrations of hydrogen peroxide. The CL measurements for each hydrogen peroxide solution were obtained in triplicates. Multiple sol-gels with immobilized quantum dots were used in this particular experiment. The results of the experiment are shown in Table 8. The mean values with the corresponding hydrogen peroxide concentrations are plotted in Figure 16.

Table 8. Results of Linearity Studies of CL Intensity with Various Concentrations of Hydrogen Peroxide Using Multiple Sol-Gels with Immobilized QD

H <sub>2</sub> O <sub>2</sub> (M)	1.75 x 10 <sup>-4</sup>	8.75 x 10 <sup>-4</sup>	1.75 x 10 <sup>-3</sup>	8.75 x 10 <sup>-3</sup>	1.75 x 10 <sup>-2</sup>
CL Intensity 1	0.0082	0.0182	0.0260	0.0670	0.0803
CL Intensity 2	0.0072	0.0171	0.0233	0.0611	0.0750
CL Intensity 3	0.0069	0.0164	0.0249	0.0642	0.0763
Mean	0.0074	0.0172	0.0247	0.0641	0.0772
RSD (%)	9.16	5.27	5.49	4.60	3.58

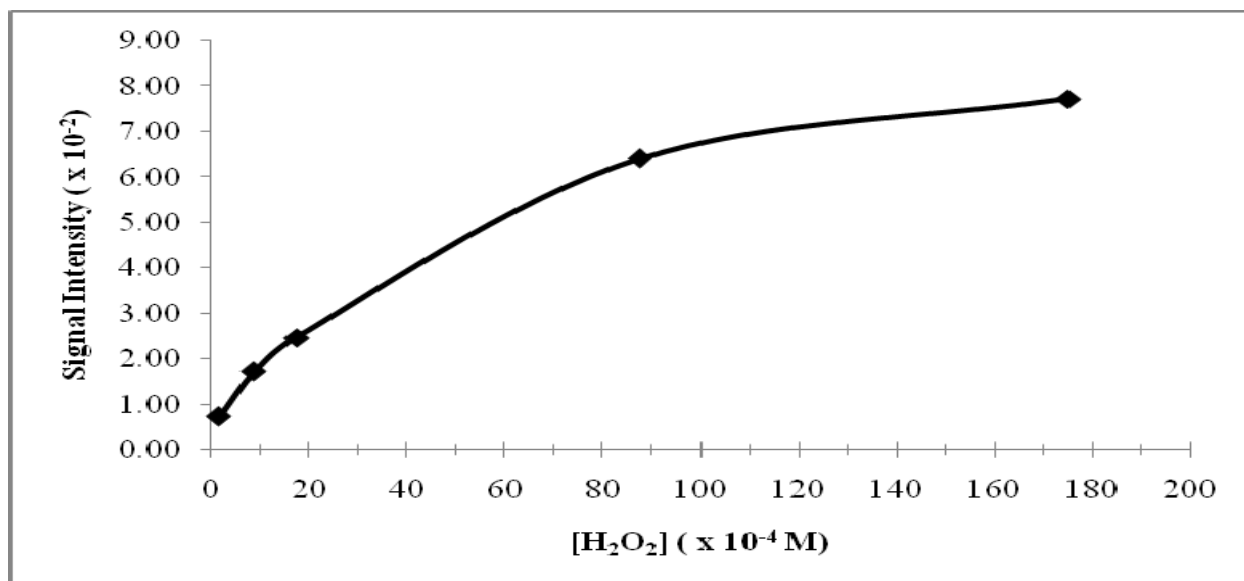


Figure 16. Plot of the average triplicate CL measurements on each hydrogen peroxide solution using 3.0 mL of TCPO, 50  $\mu$ L of imidazole, and multiple sol-gels with immobilized QD

Overall, the CL intensities of the multiple sol-gels with immobilized quantum dots were close to those of the single sol-gel with immobilized quantum dots but slightly higher with the higher hydrogen peroxide concentrations. Also, the lowest concentration of hydrogen peroxide solution gave distinctly higher RSD, though not as high as the one with the single sol-gel with immobilized quantum dots. It seems that the detection limit of the procedure was reached and the useful linear range was within  $1.75 \times 10^{-4}$  M to  $8.75 \times 10^{-3}$  M, as shown in Figure 17. In addition, using multiple sol-gels with immobilized QD does not increase the CL intensity much or help extending the dynamic range.

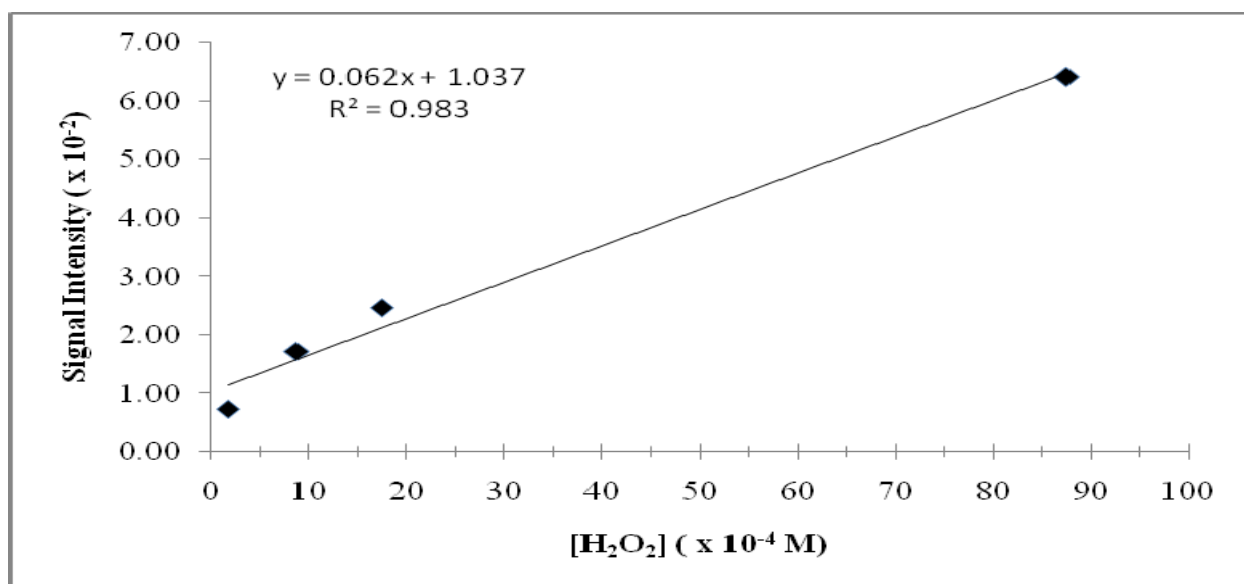


Figure 17. Plot of the linearity curve of the average triplicate CL measurements on each hydrogen peroxide solution using 3.0 mL of TCPO, 50  $\mu$ L of imidazole, and multiple sol-gels with immobilized QD. The linearity range is from  $1.75 \times 10^{-4}$  M to  $8.75 \times 10^{-3}$  M hydrogen peroxide solution.

Crushed Sol-Gels. The quantum dots located on the surface of the sol-gels were exposed to the TCPO-imidazole mixture and the hydrogen peroxide to produce a CL signal. However, it was unclear if the quantum dots well inside of the sol-gels were exposed. Therefore, the sol-gels with immobilized quantum dots were crushed into small pieces. The purpose of this experiment

was to verify if those inner quantum dots did participate in the CL reaction and if so to witness an increase in the CL intensity. The CL intensity was measured by reacting fixed volumes of TCPO and imidazole with various concentrations of hydrogen peroxide as before. The CL measurements for each hydrogen peroxide solution were obtained in duplicates. The results of the experiment are shown in Table 9. The mean values with the corresponding hydrogen peroxide concentrations are plotted in Figure 18.

Table 9. Results of Linearity Studies of CL Intensity with Various Concentrations of Hydrogen Peroxide Using Crushed Sol-Gels with Immobilized QD

H <sub>2</sub> O <sub>2</sub> (M)	3.75 x 10 <sup>-5</sup>	8.75 x 10 <sup>-5</sup>	1.75 x 10 <sup>-4</sup>	3.50 x 10 <sup>-4</sup>	1.75 x 10 <sup>-3</sup>	3.50 x 10 <sup>-3</sup>
CL Intensity 1	0.0021	0.0042	0.0050	0.0081	0.0133	0.0170
CL Intensity 2	0.0018	0.0032	0.0054	0.0069	0.0122	0.0150
Mean	0.0020	0.0037	0.0052	0.0075	0.0128	0.0160
RSD (%)	10.88	19.11	5.44	11.31	6.10	8.84

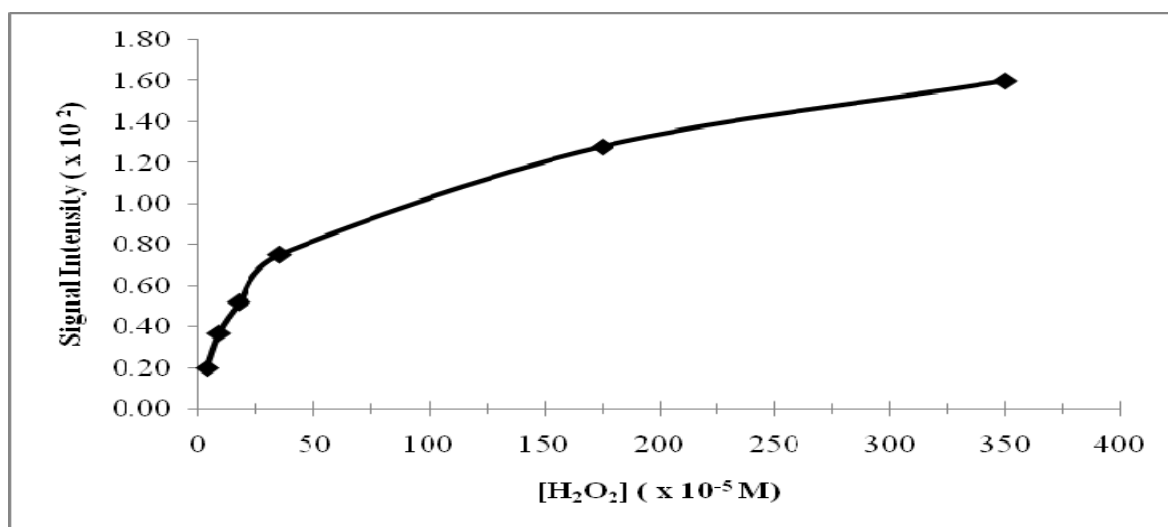


Figure 18. Plot of the average duplicate CL measurements on each hydrogen peroxide solution using 3.0 mL of TCPO, 50  $\mu$ L of imidazole, and crushed sol-gels with immobilized QD

After examining the results, the CL intensities were actually slightly less than those of the whole sol-gel with immobilized quantum dots. Thus, it seems the expectation was not met. In fact, it seems that by crushing the sol-gel with immobilized quantum dots into smaller pieces from a large one, some quantum dots were lost in the process. Thus, less fluorophore was now present. Another interesting observation was that the RSD were higher, i.e. the precision had been degraded. Additionally, it seems two slopes and a narrower linear range resulted, as shown in Figures 18, 19, and 20.

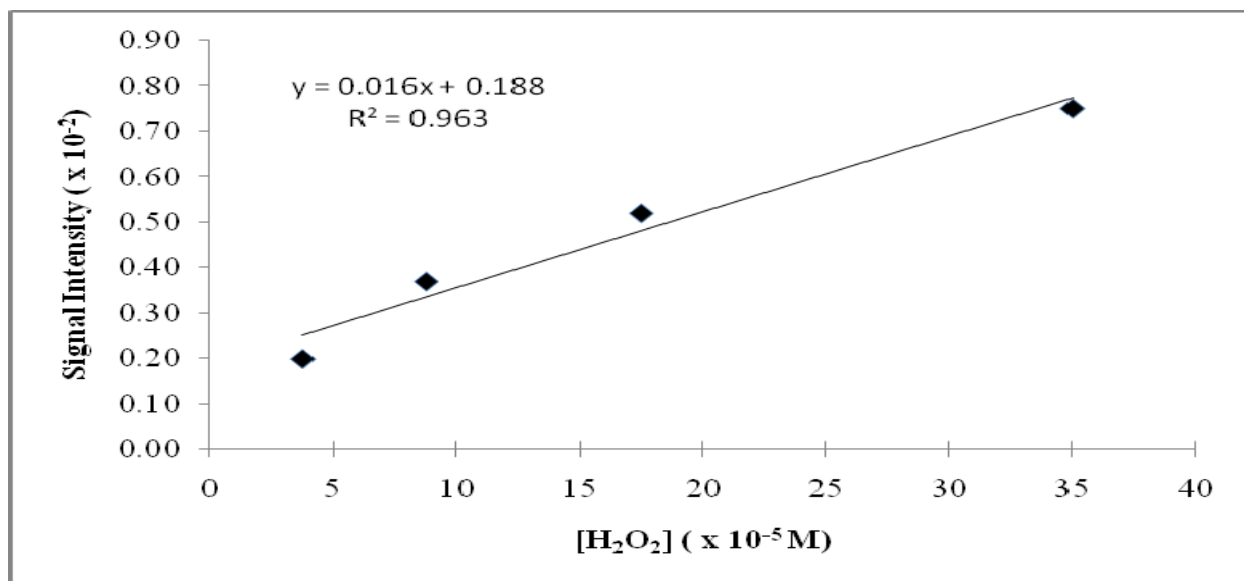


Figure 19. Plot of the linearity curve of the average duplicate CL measurements on each hydrogen peroxide solution using 3.0 mL of TCPO, 50  $\mu$ L of imidazole, and crushed sol-gels with immobilized QD. The linearity range is from  $3.75 \times 10^{-5}$  M to  $3.50 \times 10^{-4}$  M hydrogen peroxide solution.

It seems that when using crushed sol-gels with immobilized quantum dots, the linearity at the lower concentration range was somewhat extended, and the slope was greater. This means that the sensitivity of the crushed sol-gels with immobilized quantum dots was better at lower concentrations of hydrogen peroxide solution than at higher concentrations. This may be a result

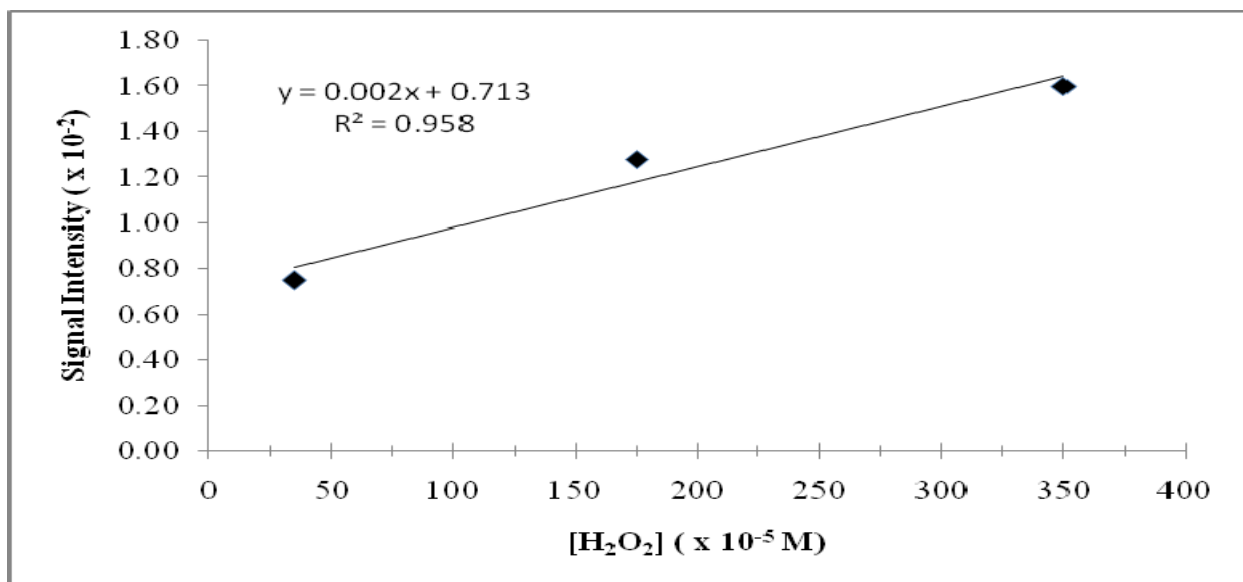


Figure 20. Plot of the linearity curve of the average duplicate CL measurements on each hydrogen peroxide solution using 3.0 mL of TCPO, 50  $\mu$ L of imidazole, and crushed sol-gels with immobilized QD. The linearity range is from  $3.50 \times 10^{-4}$  M to  $3.50 \times 10^{-3}$  M hydrogen peroxide solution.

of the presence of a large number of small particles with greater surface area leading to greater interaction and energy transfer.

## CHAPTER 5

### CONCLUSION

The synthesis and luminescence properties of CdSe quantum dots have been achieved and studied. The results obtained from all of the experiments validated the research objectives set forth. Some of the results obtained also raised more questions and require further investigation.

The proposed method for synthesizing CdSe quantum dots proved to be satisfactory. The temperature-based procedure for the synthesis of quantum dots was a great success and routine and produced quantum dots of desirable properties. The quantum dots were definitely of different sizes and progressed from a smaller size to a larger size with an increase in temperature. Similar to the time-based quantum dots, the temperature-based quantum dots emitted light ranging from the yellow to the red end of the visible spectrum. Contrary to the time-based method, the size of the quantum dots was better controlled with this method, and greater yields were obtained.

The luminescence data obtained verified the synthesis of the quantum dots and their properties. Various experiments were performed to examine the fluorescence properties of the synthesized quantum dots. For larger quantum dots, the maximum fluorescence intensity was obtained at longer emission wavelengths and vice versa for the smaller quantum dots. When excited, the fluorescence intensity of the quantum dot solution increased linearly with increase in concentration.

The immobilization of quantum dots by adsorption on chromosorb, glass bead, silica gel, and alumina surfaces was feasible but not desirable. More quantum dots of a certain size



distribution adsorbed onto the silica gel, leaving a narrower quantum dot size distribution in the solution. More quantum dots adsorbed onto the alumina of the smaller particle size than for alumina of the larger particle size. Smaller particles have larger surface areas, and, thus, more quantum dot particles can adsorb onto the surface. It is possible that better adsorption would be obtained with smaller particle sizes of any surface. However, further research would be required to verify this.

The quantum dots were successfully immobilized in sol-gels. The sol-gels with immobilized quantum dots were used as fluorophores to carry out the TCPO-CL analyses. The sol-gels with immobilized quantum dots provided reproducible data with satisfactory precision. It was proven that a single sol-gel with immobilized quantum dots could be used at least 45 times and retained its ability to luminesce over several weeks at a time. As more analyses were performed, some of the quantum dots were lost. This was evident by noting the decrease in CL intensity and the sol-gel with immobilized quantum dots losing some of its red color that was originally present before the analyses.

TCPO-CL analyses were performed using various hydrogen peroxide solutions. The luminescence data obtained were highly interesting. The CL intensity was proportional to the hydrogen peroxide concentration. The detection limit was being approached at lower concentrations, specifically  $1.75 \times 10^{-4}$  M  $\text{H}_2\text{O}_2$  solution. Thus, the useful linearity range was at higher concentrations. It was proposed that a higher CL signal could be achieved with an increase in quantum dots. Therefore, other analyses using multiple and crushed sol-gels with immobilized quantum dots were performed. The data obtained using multiple sol-gels with immobilized quantum dots showed that the CL intensities were slightly higher with higher hydrogen peroxide concentrations. However, the data obtained using the crushed sol-gels with

immobilized quantum dots proved the hypothesis to be incorrect. As the sol-gels with immobilized quantum dots were crushed, some quantum dots were lost, leaving less fluorophore in the sol-gel. Thus, the CL intensities were lower.

In conclusion, CdSe quantum dots were successfully synthesized and immobilized, and their luminescence properties were analyzed. Further studies could take place in various areas of this research. For example, the actual size of the quantum dots could be measured using a transmission electron microscope or a scanning electron microscope. In addition, more research concerning the immobilization of the quantum dots on surfaces of various particle sizes could be conducted. Finally, the two-sloped curves from the chemiluminescence analyses could be examined in more detail to accurately determine the detection limits and useful linearity range.

## REFERENCES

1. Nagarajan, R. *Nanoparticles: Synthesis, Stabilization, Passivation, and Functionalization*. **2008**, 1-14.
2. Scientific Committee on Emerging and Newly Identified Health Risks (SCENIHR). The appropriateness of existing methodologies to assess the potential risks associated with engineered and adventitious products of nanotechnologies. [http://ec.europa.eu/health/ph\\_risk/committees/04\\_scenih/ docs/scenih\\_r\\_o\\_003b.pdf](http://ec.europa.eu/health/ph_risk/committees/04_scenih/ docs/scenih_r_o_003b.pdf) (accessed March 7, 2010)
3. Shenhar, R.; Norsten, T. B.; Rotello, V. M. Polymer-mediated nanoparticle assembly: structural control and applications. *Adv. Mater.* **2005**, 17, 657-669.
4. Lin, Y. L.; Wang, T. J.; Jin, Y. Surface characteristics of hydrous silica-coated TiO<sub>2</sub> particles. *Powder technol.* **2002**, 123, 194.
5. O'Connor, J.J.; Robertson, E.F. Richard Phillips Feynman. <http://www-groups.dcs.st-and.ac.uk/~history/Biographies/Feynman.html> (accessed April 16, 2010)
6. Accelrys. Nanotechnology – the present and future – an interview with Dr. K. Eric Drexler, chairman of the foresight institute. <http://accelrys.com/resource-center/case-studies/pdf/drexler.pdf> (accessed April 16, 2010)
7. Ananthaiah, R. Discovery of fullerenes: giving a new shape to carbon chemistry. *Resonance*. **1997**, 68-73.
8. Davis, T. Biography of Louis E. Brus. *Proceedings of the National Academy of Sciences of the United States of America*. **2005**, 102 (5), 1277-1279.
9. Australian Government Department of Health and Ageing Therapeutic Goods Administration. TGA fact sheet: sunscreens. <http://www.tga.gov.au/npm/meds/sunscreen-zotd.htm#labels> (accessed May 3, 2010)
10. AZoNano – The A to Z of Nanotechnology. Silver nanoparticles – how they are providing environmentally friendly antibacterial properties in consumer goods. <http://www.azonano.com/details.asp?ArticleID=1695> (accessed May 3, 2010)

11. Nanotechnology Development Blog. Research on gold nanoparticles. <http://www.nanotechnologydevelopment.com/research/research-on-gold-nanoparticles.html> (accessed May 3, 2010)
12. Lasic, D. D. Liposomes. *Science & Medicine*. **1996**, 3 (3), 34.
13. Egbaria, K.; Weiner, N. Liposomes as a topical drug delivery system. *Advanced Drug Delivery Reviews*. **1990**, 5 (3), 287-300.
14. Loo, C.; Lowery, A.; Halas, N.; West, J.; Drezek R. Immunotargeted nanoshells for integrated cancer imaging and therapy. *Nano. Lett.* **2005**, 5 (4), 709-711.
15. Kroto, H. W.; Heath, J. R.; O'Brien, S. C.; Curl, R. F.; Smalley, R. E. C<sub>60</sub>: Buckminsterfullerene. *Nature*. **1985**, 318, 162.
16. Brus, L. E.; Bondybey, V. E. Pseudorotational local mode participation in OH and OD (A<sup>2</sup>E<sup>+</sup>) vibrational relaxation in a Ne lattice. *J. Chem. Phys.* **1975**, 63, 786-793.
17. Goodman, J.; Brus, L. E. Mechanism of vibrational relaxation in molecular solids. *J. Chem. Phys.* **1976**, 65, 3146-3152.
18. Rossetti, R.; Nakahara, S.; Brus, L. E. Quantum size effects in the redox potentials, resonance Raman spectra, and electronic spectra of CdS crystallites in aqueous solution. *J. Chem. Phys.* **1983**, 79, 1086-1088.
19. Steigerwald, M. L.; Alivisatos, A. P.; Gibson, J. M.; Harris, T. D.; Kortan, R.; Muller, A. J.; Thayer, A. M.; Duncan, T. M.; Douglass, D. C.; Brus, L. E. Surface derivatization and isolation of semiconductor cluster molecules. *J. Am. Chem. Soc.* **1988**, 110, 3046-3050.
20. Steigerwald, M. L.; Brus, L. E. Synthesis, stabilization, and electronic structure of quantum semiconductor nanoclusters. *Ann. Rev. Mater. Sci.* **1989**, 19, 471-495.
21. Yale University Science Blog. Yale scientists measure current across single organic molecule. <http://www.scienceblog.com/community/older/1997/B/199702140.html> (accessed May 1, 2010)

22. Quantum dots. (a is for...). *Science & Medicine*. **2005**, 10.2, 140.  
<http://www.sciandmed.com/sm/journalviewer.aspx?issue=1164&article=1633&action=1>  
(accessed April 18, 2010)
23. Resch-Genger, U.; Grabolle, M.; Cavaliere-Jaricot, S.; Nitschke, R.; Nann, T. Quantum dots versus organic dyes as fluorescent labels. *Nature Methods*. **2008**, 5 (9), 763-775.
24. Alivisatos, A. P. Semiconductor clusters, nanocrystals, and QDs. *Science*. **1996**, 271, 934-937.
25. Weller, H. Quantum size colloids: from size-dependent properties of discrete particles to self-organized superstructures. *Curr. Opin. Colloid Interface Sci*. **1998**, 3, 194-199.
26. Seydel, C. Quantum dots get wet. (news). (nanocrystal coatings offer protection and use of fluorescent clusters). *Science*. **2003**, 300.5616, 80-81.
27. Perkel, J. M. Quantum leap for quantum dots: researchers finally make quantum dots work for life scientists. (tools & technology). *The Scientist*. **2003**, 17.18, 46.
28. Dabbousi, B. O.; Rodriguez-Viejo, J.; Mikulec, F. V.; Heine, J. R.; Mattoussi, H.; Ober, R.; Jensen, K. F.; Bawendi, M. G. (CdSe)ZnS core-shell qds: synthesis and characterization of a size series of highly luminescent nanocrystallites. *J. Phys. Chem. B*. **1997**, 101, 9463-9475.
29. Boatman, E. M.; Lisensky, G. C.; Nordell, K. J. A safer, easier, faster synthesis for CdSe quantum dot nanocrystals. *J. Chem. Edu.* **2005**, 82 (11), 1697-1699.
30. Mason, W. T. *Fluorescent and Luminescent Probes for Biological Activity*, 2<sup>nd</sup> ed. **1999**.
31. Dahne, S.; Resch-Genger, U.; Wolfbeis, O. S., eds. *Near-infrared Dyes for High Technology Applications*. **1998**, NATO ASI Series 3, Hightechnology Vol. 52.
32. Mihindikulasuriya, S. H.; Morcone, T. K.; McGown, L. B. Characterization of acridone dyes for use in four-decay detection in DNA sequencing. *Electrophoresis*. **2003**, 24, 20-25.
33. Dahan, M.; Laurence, T.; Pinaud, F.; Chemla, D. S.; Alivisatos, A. P.; Sauer, M.; Weiss, S. Time-gated biological imaging by use of colloidal QDs. *Opt. Lett.* **2001**, 26, 825-827.

34. Grecco, H. E.; Lidke, K. A.; Heintzmann, R.; Lidke, D. S.; Spagnuolo, C.; Martinez, O. E.; Jares-Erijman, E. A.; Jovin, T. M. Ensemble and single particle photophysical properties (two-photon excitation, anisotropy, FRET, lifetime, spectral conversion) of commercial quantum dots in solution and in live cells. *Microsc. Res. Tech.* **2005**, 65, 169-179.
35. Rhyner, M. N.; Smith, A. M.; Gao, X.; Mao, H.; Yang, L.; Nie, S. Quantum dots and multifunctional nanoparticles: new contrast agents for tumor imaging. *Nanomedicine.* **2006**, 1.2.
36. Schlegel, G.; Bohnenberger, J.; Potapova, I.; Mews, A. Fluorescence decay time of single semiconductor nanocrystals. *Phys. Rev. Lett.* **2002**, 88, 137401.
37. Zhang, K.; Chang, H.; Fu, A.; Alivisatos, A. P.; Yang, H. Continuous distribution of emission states from single CdSe/ZnS QDs. *Nano. Lett.* **2006**, 6, 843-847.
38. Curtis, A.; Wilkinson, C. Nanotechniques and approaches in biotechnology. *Trends Biotechnol.* **2001**, 19, 97-101.
39. Gref, R.; Minamitake, Y.; Peracchia, M. T.; Trubetskoy, V.; Torchilin, V.; Langer, R. Biodegradable long-circulating polymeric nanospheres. *Science.* **1994**, 263, 1600-1603.
40. Lagally, M. G. Self-organized quantum dots. *J. Chem. Edu.* **1998**, 75 (3), 277-279.
41. Campbell, D. J.; Lorenz, J. K.; Ellis, A. B.; Kuech, T. F.; Lisensky, G. C.; Whittingham, S. The computer as a materials science benchmark. *J. Chem. Edu.* **1998**, 75, 297-312.
42. Pejova, B.; Tanusevski, A.; Grozdanov, I. Chemical deposition of semiconducting cadmium selenide quantum dots in thin film form and investigation of their optical and electrical properties. *J. Solid State Chemistry.* **2003**, 172, 381-388.
43. Jin, W. J.; Costa-Fernandez, J. M.; Pereiro, R.; Sanz-Medel, A. Surface-modified CdSe quantum dots as luminescent probes for cyanide determination. *Analytica Chimica Acta.* **2004**, 522, 1-8.
44. Murphy, C. J. Peer reviewed: optical sensing with quantum dots. *Anal. Chem.* **2002**, 74, 521A.

45. Hutchins, B. M.; Morgan, T. T.; Ucak-Astarlioglu, M. G.; Williams, M. E. Optical properties of fluorescent mixtures: comparing quantum dots to organic dyes. *J. Chem. Edu.* **2007**, 84 (8), 1301-1303.
46. Bognolo, G. The use of surface-active agents in the preparation and assembly of quantum-sized nanoparticles. *Advances in Colloid and Interface Science.* **2003**, 106, 169-181.
47. Palgrave, R. G.; Parkin, I. P. Aerosol assisted chemical vapor deposition using nanoparticle precursors: a route to nanocomposite thin films. *J. Am. Chem. Soc.* **2006**, 128, 1587-1597.
48. Murray, C. B.; Norris, D. J.; Bawendi, M. G. Synthesis and characterization of nearly monodisperse CdE (E = sulfur, selenium, tellurium) semiconductor nanocrystallites. *J. Am. Chem. Soc.* **1993**, 115, 8706-8715.
49. Liu, F.; Lagally, M. G. Self-organized nanoscale structures in Si/Ge films. *Surf. Sci.* **1997**, 386, 169.
50. Chan, W. C. W.; Nie, S. M. Quantum dot bioconjugates for ultrasensitive nonisotopic detection. *Science.* **1998**, 281, 2016-2018.
51. Gao, X. H.; Nie, S. M. Doping mesoporous materials with multicolor quantum dots. *J. Phys. Chem. B.* **2003**, 107, 11575-11578.
52. Han, M. Y.; Gao, X.; Su, J. Z.; Nie, S. Quantum-dot-tagged microbeads for multiplexed optical coding of biomolecules. *Nat. Biotechnol.* **2001**, 19, 631-635.
53. Vossmeier, T.; Katsikas, L.; Giersig, M.; Popovic, G.; Diesner, K.; Chemseddine, A.; Eychmueller, A.; Weller, H. CdS nanoclusters: synthesis, characterization, size dependent oscillatory strength, temperature shift of the excitonic transition energy, and reversible absorbance shift. *J. Phys. Chem.* **1994**, 98, 7665-7673.
54. Peng, X.; Manna, L.; Yang, W.; Wickham, J.; Scher, E.; Kadavanich, A.; Alivisatos, A. P. Shape control CdSe nanocrystals. *Nature.* **2000**, 404, 59-61.
55. Puntès, V. F.; Krishnan, K. M.; Alivisatos, A. P. Colloidal nanocrystal shape and size control: the case of cobalt. *Science.* **2001**, 291, 2115-2117.

56. Skoog, D. A.; Holler, F. J.; Crouch, S. R. *Principles of Instrumental Analysis*, 6<sup>th</sup> ed. Thomson Higher Education: Belmont, CA, **2007**, 399-425.
57. Gopal, M.; Moberly Chan, W. J.; De Jonghe, L. C. Room temperature synthesis of crystalline metal oxides. *J. Mater. Sc.* **1997**, 32, 6001-6008.
58. Mohan, A. G.; Turro, N. J. A facile and effective chemiluminescence demonstration experiment. *J. Chem. Ed.* **1974**, 51, 528.
59. Rauhut, M. M.; Roberts, B. G.; Semsel, A. M. A study of chemiluminescence from reactions of oxalyl chloride, hydrogen peroxide, and fluorescent compounds. *J. Am. Chem. Soc.* **1966**, 88, 3604.
60. Bollyky, L. J.; Whitman, R. H.; Roberts, B. G.; Rauhut, M. M. Chemiluminescence from reactions of oxalic anhydrides with hydrogen peroxide in the presence of fluorescent compounds. *J. Am. Chem. Soc.* **1967**, 89, 6523.
61. Rauhut, M. M.; Bollyky, L. J.; Roberts, B. G.; Loy, M.; Whitman, R. H.; Iannotta, A. V.; Semsel, A. M.; Clarke, R. A. Chemiluminescence from reactions of electronegatively substituted aryl oxalates with hydrogen peroxide and fluorescent compounds. *J. Am. Chem. Soc.* **1967**, 89, 6515.
62. Sherman, P. A.; Holzbecher, J.; Ryan, D. E. Analytical applications of peroxyoxalate chemiluminescence. *Analytica Chimica Acta.* **1978**, 97, 21.
63. Williams III, D. C.; Huff, G. F.; Seitz, W. R. Evaluation of peroxyoxalate chemiluminescence for determination of enzyme generated peroxide. *Anal. Chem.* **1976**, 48, 1003.
64. Ponten, E.; Stigbrand, M.; Irgum, K. Immobilized amino aromatics for solid-phase detection using imidazole-mediated bis(trichlorophenyl) oxalate chemiluminescence. *Analytical Chemistry.* **1995**, 67, 4302.
65. Shukla, N.; Nigra, M.M. Synthesis of CdSe quantum dots with luminescence in the violet region of the solar spectrum. *Luminescence: The Journal of Biological and Chemical Luminescence.* **2010**, 25, 14-18.



66. Qingwen L.; Guoan, L.; Yiming, W.; Xingrong, Z. Immobilization of glucose oxidase in sol-gel matrix and its application to fabricate chemiluminescent glucose sensor. *Materials Science and Engineering*. **2000**, 11 (1), 67-70.

## VITA

### TRAVIS JUSTIN HEATH

Personal Data:                   Date of Birth: June 4, 1986  
  Place of Birth: Bristol, Virginia  
  Marital Status: Single

Education:                        Virginia Polytechnic Institute and State University (Virginia Tech)  
  Blacksburg, Virginia, Chemistry, B.S. 2008  
  East Tennessee State University (ETSU)  
  Johnson City, Tennessee, Chemistry, M.S. 2010

Achievements:                   Outstanding Teaching Assistant Award, 2008-2009

Professional Experience:       Employee of Global Coatings Applications Development team at  
  Eastman Chemical Company  
  Kingsport, Tennessee, 2004  
  Polymer Lab Analyst at Eastman Chemical Company  
  Kingsport, Tennessee, 2006-2008  
  Graduate Teaching Assistant at ETSU  
  Johnson City, Tennessee, 2008-2010